A Laboratory Study of the Effects of Organic Solvents On the Physical Properties of Ca-smectite and Clay-Dominated Systems

By Paul S. Domski

A Thesis Submitted In Partial Fulfillment of the
Requirements of the Master of Science Degree In
Geochemistry

New Mexico Institute of Mining and Technology

June, 1989

ACKNOWLEDGMENT

ABSTRACT

The effects of organic solvents on the physical properties of two clays, one the aquitard material from the SJ-6 Superfund site in Albuquerque, New Mexico, and the other a reference Ca-smectite from the Clay Minerals Repository were investigated. The investigation took a two step approach: in Phase One the crystalline swelling characteristics of the two clays saturated with organic compounds were investigated using X-ray diffraction techniques; and in Phase Two of the experiment, closed cell permeameters were used to monitor the hydraulic conductivity of the bulk clay material from the SJ-6 Superfund site to determine how the hydraulic properties respond to the addition of dissolved trichloroethene (TCE) and pure TCE, and whether TCE can cause macropores to form.

The results of the investigation reveal that relative to the swelling caused by water, all the organic compounds cause collapse of the crystal lattice of the smectite fraction of the two experimental clays in the c-dimension. The properties of the organic liquid which best predict the organic's effect on the c-dimension of the smectite fraction are the compound's dielectric constant, which has a correlation of $r = 0.74$, and the compound's log n-octanol-water partition coefficient (log K_{ow}) which has a negative correlation of $r = -0.83$. The interparticle distance of the non-expanding lattice clays (illite and kaolinite) of the SJ-6 material was altered by some of the organic compounds. Aqueous dilutions of TCE did not cause any significant alteration of the hydraulic conductivity of the clay material from the SJ-6 site. Pure TCE was not able to flow through the clay material due to the extreme capillary pressure required to replace pore water with TCE, and macropore formation did not occur.

Implications of this study are that organic compounds have the potential to alter the physical dimensions of clay minerals, and thus alter the hydraulic properties of clay dominated systems.

TABLE OF CONTENTS

LIST OF FIGURES

LIST OF TABLES

CHAPTER 1

INTRODUCTION

Land disposal of toxic waste by our predecessors has affected the quality of our national water resources. Concerns about further contamination of groundwater resources arise from the fact that 50 percent of our nations population depends on groundwater as its primary source of drinking water (Office of Technology Assessment, 1984). Public health concerns arise because many contaminants have been linked to cancers, liver and kidney damage, and damage to the central nervous system. Further, the unknown effects, particularly the long term effects, of exposure to low levels of contamination are a cause of much public anxiety.

The old practice of "backdoor" disposal of spent industrial solvents and secondary processing wastes to the ground surface and shallow unlined pits with the belief that they will degrade to harmless substances before reaching the water table is now known to be unsafe (Office of Technology Assessment, 1984). Due to the limited ability of the soil column to render toxic substances harmless, extensive disposal guidelines must be employed to prevent further contamination of our nation's groundwater.

Clay-lined surface impoundments are a common means of reducing and concentrating large volumes of waste generated at industrial sites. Many states currently require the hydraulic conductivity of such liners not exceed 10^{-7} cm/s (Anderson and Brown, 1981). The regulations, however, do not specify the type of permeant used in determining hydraulic conductivity. In most studies hydraulic conductivities are determined using 0.01N $CaCl_2$ or $CaSO_4$ solution which

bears little resemblance to the leachate released from disposed liquids and sludges (Anderson and Brown, 1981).

Fluids of varying dissolved solids concentration (TDS), and those containing organic wastes are known to change the hydraulic character of clay dominated systems (Anderson and Brown, 1981; Green et al., 1981; Schramm et al., 1986; Shainberg et al., 1988). The mechanism responsible is the expansion or contraction of the crystal lattice of the expanding–lattice clay mineral groups, smectite and vermiculite, and mixed–layer illite-smectite (I/S), and the change in the interparticle distance of the non–expanding clay mineral groups, illite and kaolinite. Processes controlling crystalline swelling are: 1) ionic exchange of the interlayer cation for one of a different valence, 2) dispersion of the clay by low TDS water, and 3) replacement of the interlayer water with a fluid of differing chemical properties (Shainberg et al., 1988; Brindley et al., 1969). The physical alteration of the of crystallographic dimensions results in a bulk change in the volume of the clay fraction causing a proportional change of the pore dimensions of the media. Before a clay material can be approved for use as a liner several tests should be performed (e.g., hydraulic conductivity and consolidation tests) to evaluate how the clay material reacts to a variety of chemical environments, e.g., variable TDS water and common organic contaminants.

The small particle size and the sheet structure of clay minerals produces a very high surface–area–to–volume ratio which renders a clay dominant system highly chemically reactive relative to a clay poor system. Due to the reactive nature of clay–rich systems the physical properties of the system can be readily altered by the chemistry of the surrounding environment. As the physico-chemical behavior of a clay liner can be predicted from laboratory studies so it can for clay–rich geologic horizons which are supposed barriers to the transport

of contaminants to the groundwater. The hydraulic properties of an aquitard in areas of known contamination may be modified by the contaminated fluids such that flow may occur between zones which were at one time isolated by the aquitard.

SCOPE AND OBJECTIVE

In the current study the clay material of a shallow aquitard at the San Jose Superfund site of Albuquerque's South Valley, a site of known contamination by organic chemicals, was investigated with regard to how it responded to a number of organic chemicals. The investigation incorporated a two-stage experimental approach. The first stage used X-ray diffraction techniques to gain an understanding of the intracrystalline swelling properties of the smectite fraction of the clay minerals in the presence of organic chemicals of differing properties; the second stage employed a column study to establish the relative hydraulic conductivity of the clay material and how it was affected by the organic chemical trichloroethene (TCE), and to observe whether TCE caused the formation of cracks or *macropores*.

Graphical analysis provided a means of relating the intracrystalline swelling characteristics of the smectite fraction of the clay minerals to the chemical properties of the organic compounds. From these relationships a basic understanding of how the organic chemical's properties affected the crystallographic dimensions of smectite was obtained.

BACKGROUND INFORMATION

SITE INFORMATION

The following summation of site information, site geology, and site hydrogeology was taken from drafts of Remedial Investigation reports (on file at

the Public Works Office of the City of Albuquerque) submitted to the U.S. Environmental Protection Agency, New Mexico Environmental Improvement Division (NMEID), and the City of Albuquerque by Hart Associates Inc., and by Black and Veatch Consulting Engineers as part of the Superfund process.

LOCATION

The SJ–6 Superfund site is in the South Valley of Albuquerque, Bernalillo County, New Mexico (Fig. 1–1). The site, of less than one square mile in area, is within an industrial– and residential–zoned area. The exact surface boundary of the contaminated area is difficult to define so property lines rather than the groundwater capture zone of the SJ–6 municipal well defines the study area.

INDUSTRIAL HISTORY

Industrial development in the South Valley area began in the late 1940's, and continues through today. Early industries occupying the site were at first metal parts and heavy equipment manufacturers, which were followed by petroleum handling and storage facilities, and the last businesses to move on to the site were handlers of a wide range of chemical products including petroleum products. All of the industries mentioned are still active at the site to some degree.

The first industries to occupy the SJ–6 area created wastes associated with such activities as welding, metal plating, machining metal parts, and welding and machining plastics. These wastes might include substances such as high TDS waters, and organic solvents used to clean metal parts. Wastes created from these industries met with uncertain fate because records were rarely kept (Black and Veatch Consulting Engineers, 1988).
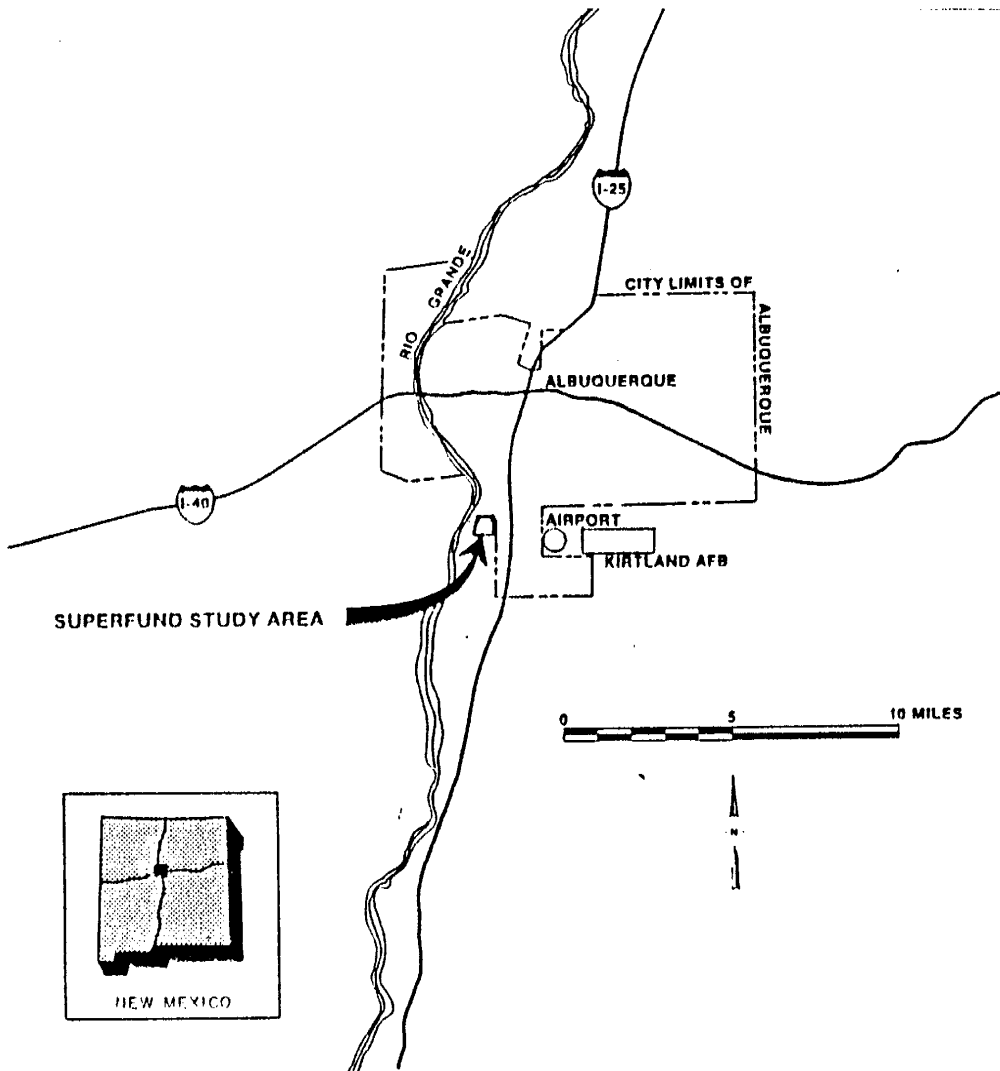
Figure 1-1. LOCATION MAP OF THE SJ-6 SITE (after Black and Veatch Consulting Engineers, 1988)

By the mid–1950's petroleum products were being received by Chevron and Texaco via underground pipelines. These facilities functioned as transfer points for local distribution of bulk petroleum products, and for Chevron, also as a storage area for prepackaged petroleum products which were sold at local retail outlets (Black and Veatch Consulting Engineers, 1988).

Chevron's waste management policy included the disposal of waste to the ground's surface. These wastes included water separated from bulk petroleum products, and materials purged from tank trucks and barrels using either high-pressure water or organic solvents. Chevron also conducted fire prevention exercises by pouring gasoline and diesel fuel on the ground surface where upon ignition the fire was extinguished with fire fighting solutions.

The other companies at the site include Duke City, Whitfield, and the Edmunds Street Property which has had several industries in occupancy (Fig. 1-2). Duke City handles and repackages petroleum and related automotive products. Whitfield cleaned, refueled, and repaired tank trucks. The Edmunds Street Property has been used for industrial and commercial purposes for the last 20 years. All three of these facilities have practiced questionable waste management policies which could lead to soil and groundwater contamination.

REGIONAL GEOLOGIC SETTING

The following discussion of the Albuquerque Basin is after Kelly (1977), unless otherwise cited. The SJ-6 Superfund site lies within the Albuquerque Basin of central New Mexico (Fig. 1-3). The Albuquerque Basin is a structural basin located along the Rio Grande valley approximately centered in the state. The Albuquerque Basin is one of a long line of basins or troughs along the Rio
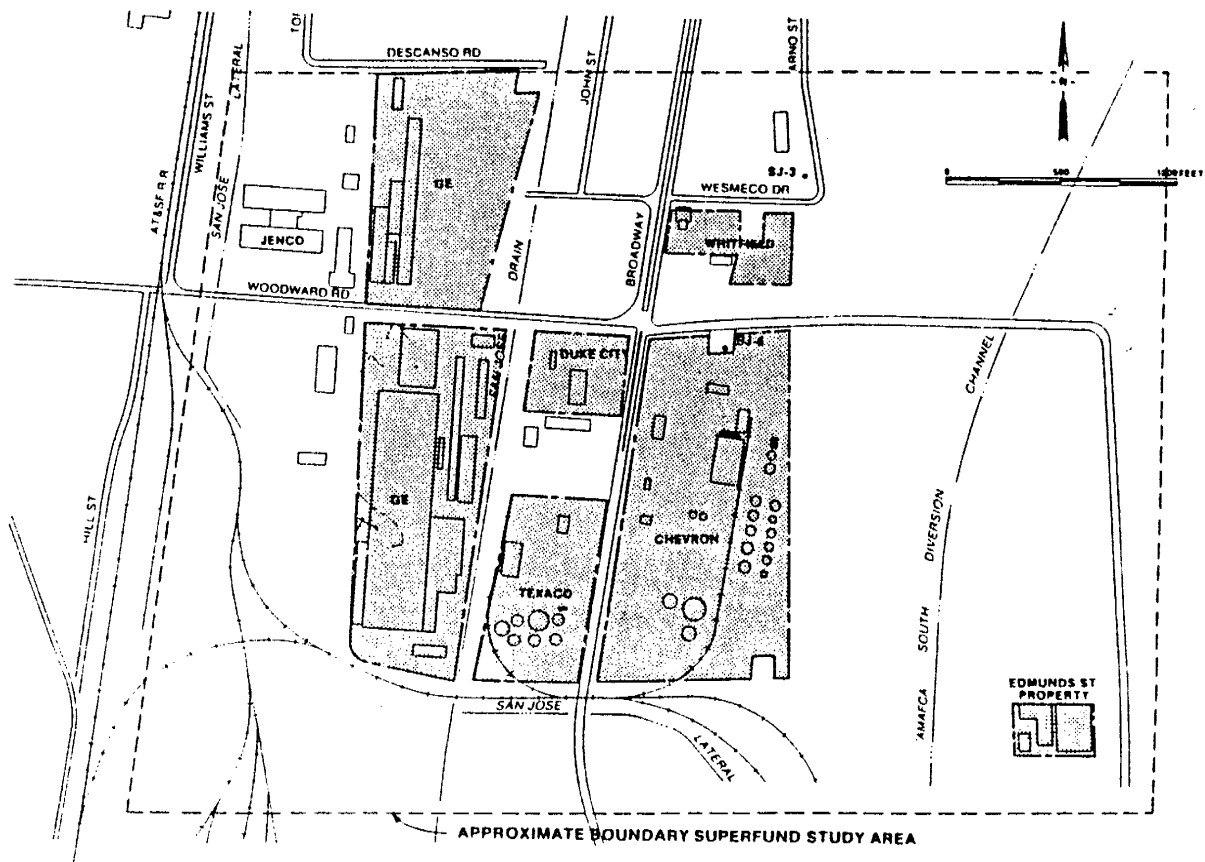
FIGURE 1–2. SJ–6 SUPERFUND STUDY AREA (after Black and Veatch Consulting Engi-

neers, 1988).

8
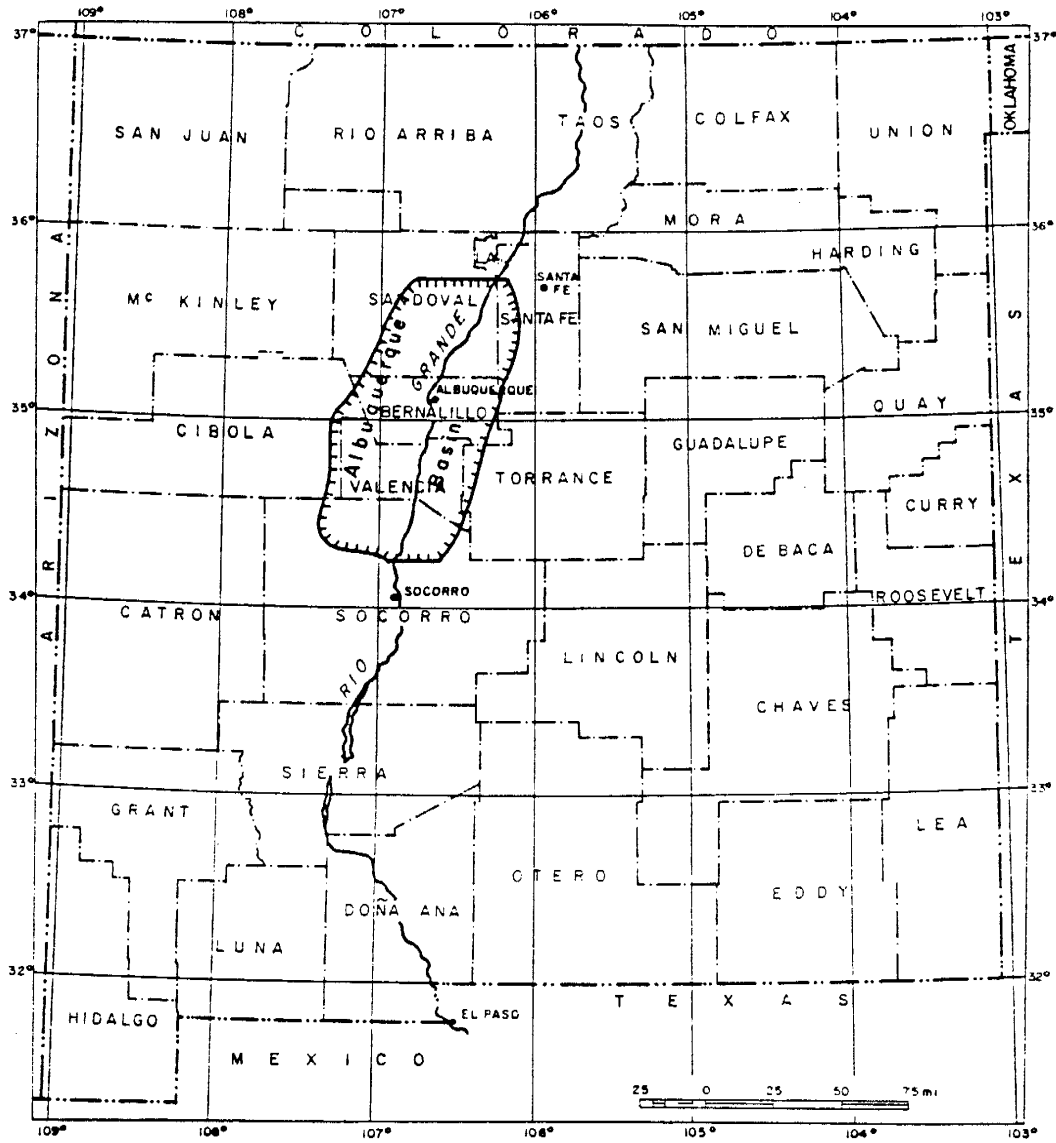
FIGURE 1-3. Location Map of the Albuquerque Basin (Kelly, 1977)

Grande collectively termed the Rio Grande depression by Kirk Bryan in 1938. This depression was named because the Rio Grande drainage follows the intermontane basins through most of their known extent. The western boundary of the Albuquerque Basin is formed by the Colorado Plateau and the southern end of the Nacimiento uplift. While the eastern boundary is comprised of the Sandia, Manzano, and Los Pinos fault blocks. The northern terminus is formed in part by the broadening of the Nacimiento uplift into the Jemez uplift, and in part by convergence of the La Bajada fault scarp with the Jemez uplift. The southern terminus of the basin is the Socorro constriction.

Rocks of the Albuquerque Basin range in age from Precambrian to Holocene. Precambrian, Paleozoic, Mesozoic and early Tertiary rocks primarily out crop at the uplifted basin margins with minor intrabasin outcrops exposed at structural highs. Mid–Miocene and younger rocks comprise the basin fill formations, and consist of the Sante Fe Group. The Sante Fe Group unconformably overlies prebasin deposits which include terranes ranging from Eocene to Precambrian in age. Deposition of 3700 meters of sediment of the Santa Fe continued through the late Pliocene. The sediments can be characterized as a bolson deposit comprised of fanglomerate, playa, fluvial, and eolian facies typical of rift basins with an axial river, and are unconsolidated to moderately consolidated with particle sizes ranging from boulders to clay.

Late Pliocene tectonism widened the basin, elevated the uplands, and deformed the Sante Fe Group, thus marking the end of Santa Fe deposition (Chapin, 1980). Post–Santa Fe deposition in the Albuquerque Basin can be characterized by alluvial, fluvial, and eolian processes. Typically, alluvial fans abut the uplifted fault blocks at the margins of the basin, grading basinward into finer sediments which interfinger with floodplain alluvium of the inner valley of

the Rio Grande. Towards the toe of the fans sediment is available for eolian transport resulting in blankets of wind deposited sand on the preexisting alluvial features. These recent deposits unconformably overlie the Sante Fe Group, and are comprised of up to 60 meters of unconsolidated sediment ranging in size from clays to boulders.

REGIONAL HYDROGEOLOGY

The important water–bearing stratigraphic units in the Albuquerque Basin are the Sante Fe Group and the Quaternary alluvium (Titus, 1982). The relatively high hydraulic conductivity combined with the great thickness of the deposits render the basin a huge groundwater reservoir. The reservoir is bounded by the highlands along the basin margin, and from below, by low permeability geologic units. Units within the valley fill are typically in hydraulic communication, although both perched and confined aquifer conditions are known to exist. These conditions reflect the large–scale heterogeneities in the aquifer system and the complexity of the spatial distribution of facies in the aquifer.

Pumping yields of wells screened in the Santa Fe range from a few gallons to thousands of gallons per minute (Titus, 1982). Wells screened in the alluvial deposits have pumping rates that range from 200 to 2000 gallons per minute (Titus, 1982). Both the Santa Fe and the alluvial aquifers are saturated through their entire thickness. The depth to water in most areas, for the alluvial aquifer is less than three meters (Titus, 1982).

Recharge of the valley fill aquifers occurs via infiltration at the basin margin highlands, from surface water sources, and ground water inflow from outside the basin. The Sandia mountains receive up to 80 cm of annual precipitation, much of which is available for recharge along the arroyos which drain the mountains (Kelley, 1977). The Rio Grande, irrigation canals, and surface

impoundments serve as sources of recharge (Hart Associates Inc., 1988). The valley aquifers discharge by the mechanisms of evaporation, transpiration, drain flow, well pumpage, and discharge to the Rio Grande (Titus, 1982).

SITE GEOLOGY AND HYDROGEOLOGY

The stratigraphy of the SJ-6 site is complex and reflects the transition from an alluvial to a fluvial depositional environment of the inner valley (Fig. 1-4 and 1-5). Three water-bearing zones are present below the study area (Black and Veatch Consulting Engineers, 1988; Hart Associates Inc., 1988). These zones are described as follows:

1) A shallow water-bearing zone which correlates to the uppermost sands and gravels of the recent floodplain deposits of the Rio Grande. This zone is continuous throughout the study area and most of the South Valley area. Depth to water in the shallow zone was historically about 1-2 meters below the ground surface. Since the installation of a drain system in 1927 and an increased demand for irrigation water the phreatic surface has been depressed an additional 1-5 meters (3-6 meters below the ground surface). Direction of groundwater flow in the shallow zone is generally toward the south, but local pumping and groundwater mounding may alter flow directions (Hart Associates Inc., 1988).

This unit was present in all of the cores obtained from the NMEID (henceforth called "SV cores") at depths from 0-4 meters below the surface. Particle size analysis of this layer are typically in the range; sand and larger 70-90%, silt 20-30%, and clay 1-10%. The clay mineralogy of the <2μm fraction of this unit is characterized by kaolinite 3-5/10, Ca-smectite 2-4/10,
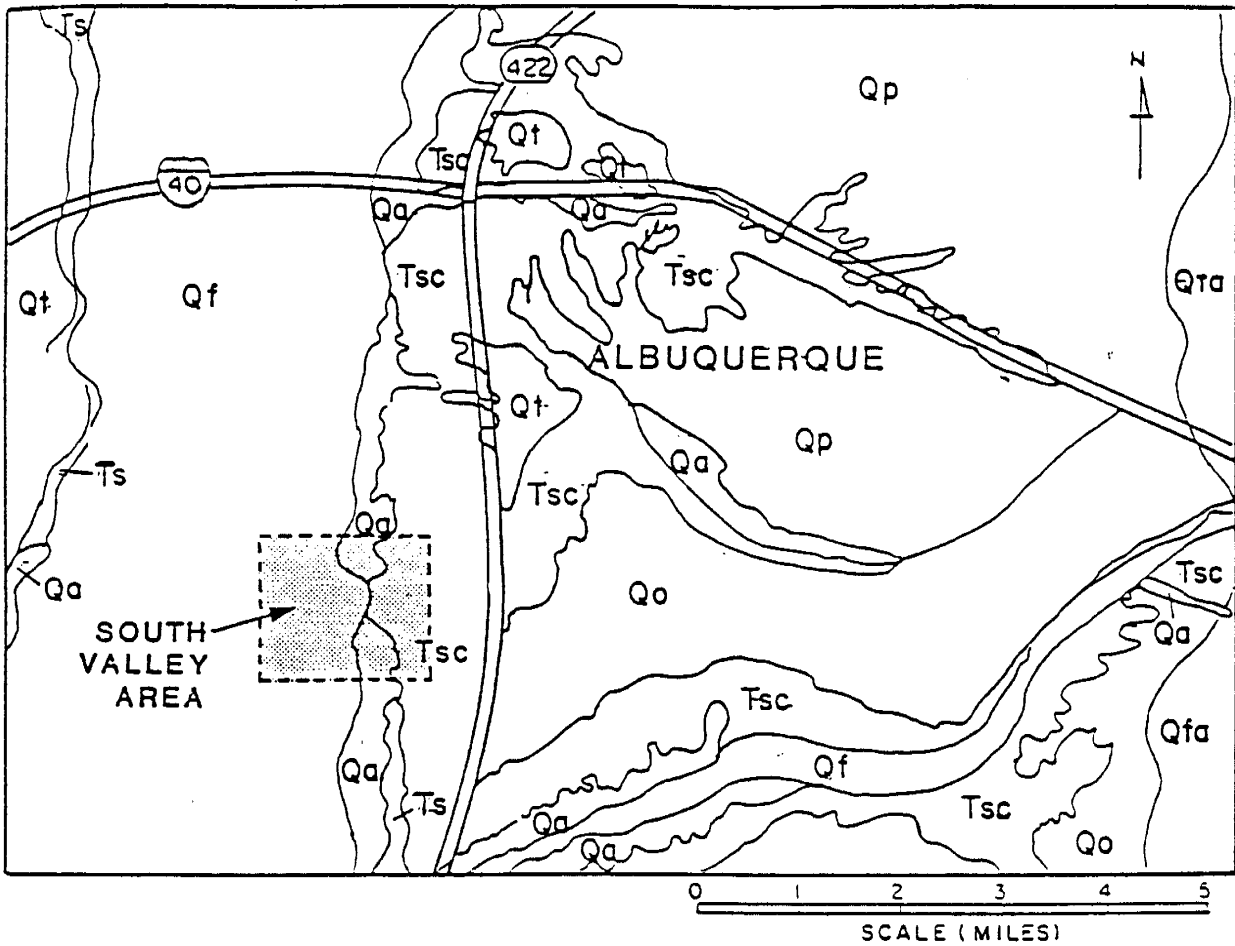
L E G E N D

Qa   ARROYOS ALLUVIUM

Qfa   FANS ALLUVIUM

Qf   FLOODPLAINS ALLUVIUM

Qt   GRAVEL TERRACES

Qp   GRAVEL PEDIMENTS

Qo   ORTIZ PEDIMENT GRAVEL AND SURFACE

Ts   SANTA FE FORMATION UNDIVIDED

Tsc   CEJA MEMBER OF SANTA FE
      FORMATION

Figure 1-4. Geologic Map of the Area Adjacent to the Sj-6 Site (after Kelly, 1977).

3-9 m — Shallow zone comprised of the upper most sands and gravels of recent flood plain deposits of the Rio Grande.

3-5 m — Discontinuous clay-silt aquitard.

15-20 m — Intermediate zone comprised of sands, gravels, and cobbles of the basal floodplain alluvium in the western portion of the study area, and the Ceja Member of the Santa Fe Group in the east.

1000's m — Deep zone comprised of clays, silts, sands, and gravels of the Santa Fe Group.

KEY

Clay-Silt
Fine Sand
Sand
Gravel
Cobbles

Figure 1-5. SCHEMATIC STRATIGRAPHIC COLUMN OF THE SJ-6 AREA.

I/S 1–3/10, and illite 1–2/10.

2) An intermediate depth water–bearing zone exists, and underlies the entire South Valley area (Hart Associates Inc., 1988). This aquifer is comprised of basal floodplain alluvium in the western portion of the study area and of the Ceja member of the Sante Fe Group in the eastern portion of the study area. The average depth to the top of this zone is about 25 meters but varies as a function of the ground surface elevation. The intermediate zone is wedge shaped and thickens from 5–10 meters in the west to 12–20 meters in the east beneath the study area. Groundwater in this zone is present in semi–confined conditions due to the presence of a discontinuous clay–silt aquitard which sepa-rates the shallow zone from the intermediate zone. The discontinuous nature of the aquitard allows hydraulic communication between these two zones providing pathways for the transport of contaminants between zones (Hart Associates Inc., 1988).

The discontinuous aquitard, which is the material under investigation in this study, was present in five of the seven SV cores, and occurred at depths ranging from 2–5 meters below the surface. Particle size analyses reveals that this unit is clay dominant; clay 40–60%, silt 20–30%, and sand and larger 5–15%. The clay mineralogy of the <2μm fraction of the aquitard is typically; kaolinite 3/10, smectite 2–3/10, I/S 1–3/10, and illite 2/10. Due to its close proximity to the river and its fine–grained character, the aquitard is most likely to be an overbank deposit of the Ancestral Rio Grande.

The intermediate aquifer is represented in one of the seven SV cores from NMEID, and occurs in the depth interval from 27–36 meters. The sedi-ments of this unit are primarily sand–to–silty sand, and the clay mineralogy of

the <2µm fraction are, kaolinite 2-3/10, smectite 1-3/10, I/S 0-2/10, and illite 1-2/10.

3) High yield municipal wells are completed in the deep-zone aquifer which occurs in the Sante Fe Group. This aquifer underlies the entire study area and much of the city of Albuquerque, and is hundreds of meters thick, consisting of interfingering deposits of sands, silts, clays, and gravels. The top of the Santa Fe aquifer and the base of the intermediate zone are in hydraulic communication as no continuous confining layer exists between them. However, layers of clay and cemented silt horizons below the contact of the deep and intermediate zones act as discontinuous aquitards resulting in the majority of the deep-zone Sante Fe Group's groundwater to be under semi-confined conditions (Black and Veatch Consulting Engineers, 1988). The deep zone aquifer was not represented in any of the SV cores from the NMEID because none of wells were completed at the necessary depth. Historically, groundwater flow in the Santa Fe formation was toward the southwest, but with increased water demands of the city of Albuquerque pumpage of the municipal wells has resulted in a reversal of hydraulic gradient and flow is now in a northeasterly direction.

CLAY COLLOID CHEMISTRY

STRUCTURE OF CLAY MINERALS

The following description of the structure of clay minerals and their characteristics is from Guven (1988), unless otherwise noted.

The clay minerals considered in this study are phyllosilicates, and are composed of either one or two, two-dimensional *tetrahedral* sheets of the composition T_2O_5 (T= tetrahedral cation, normally Si^{4+}, with Al^{3+} and Fe^{3+} com-

monly substituting), in which three basal oxygens are shared with neighboring tetrahedra to form a hexagonal mesh pattern in the a and b crystallographic directions. The apices of each tetrahedra point toward the adjacent *octahedral* sheet, in the c–direction, where the bonding plane between sheets consists of apical oxygens of the tetrahedral sheet and hydroxyl groups, of the octahedral sheet, which lie at the center of each tetragonal 6–fold ring. The unit cell of an octahedral sheet consists of three octahedra which are linked laterally by sharing octahedral edges. If two of the three octahedral sites are occupied by trivalent cations the sheet is classified *dioctahedral*. If three of the octahedral sites in the unit cell are occupied by predominantly divalent cations, the sheet is classified *trioctahedral*.

The two fundamental structural units of phyllosilicates, the tetrahedral and octahedral sheets, can take either of two configurations. The 1:1 configuration is composed of one tetrahedral and one octahedral sheet where the hydroxyl groups of the octahedra are replaced by the apical oxygens of the tetrahedra, and the unshared plane of anions on the octahedral sheet consists entirely of hydroxyl groups (Fig. 1–6a). Isomorphous substitution may occur in either of the two component layers of 1:1 structures, but overall electroneutrality must be maintained in the crystal lattice (Guven, 1988). Giese (1988) states, "Unlike the micas, smectites and vermiculites, the layer of the kaolin–group minerals has either no charge or, at most, a very small one."

The 2:1 configuration consists of two tetrahedral sheets and one octahedral sheet where the octahedral sheet is sandwiched between the inward pointing apices of the tetrahedral sheets (Fig. 1–6b). Both anion planes of the octahedral sheet in 2:1 structures consist of the same O–OH composition.
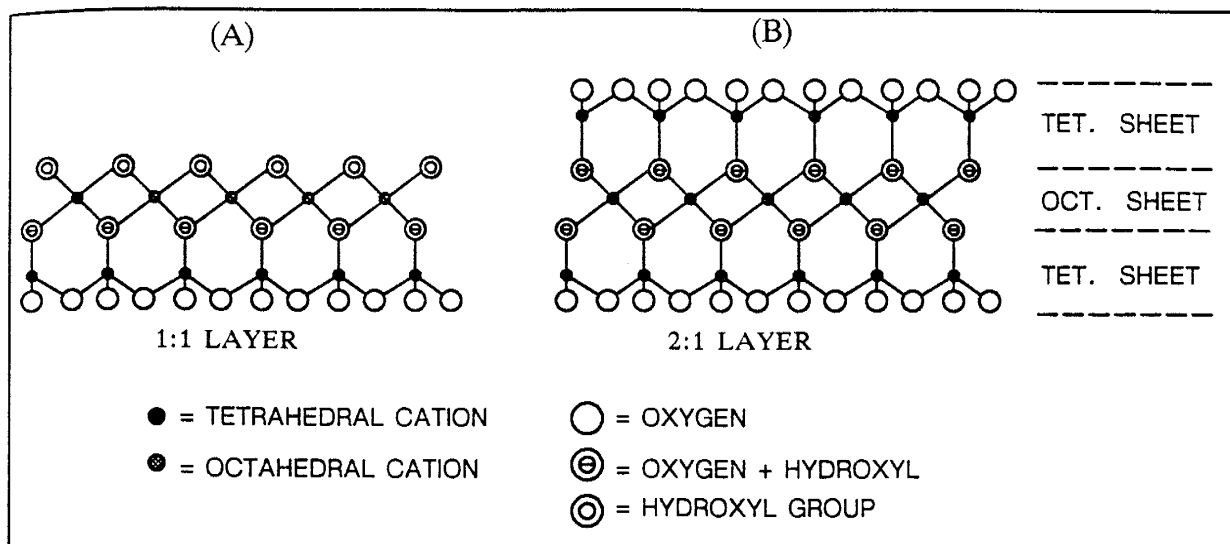
Figure 1-6. SCHEMATIC OF (A)1:1, AND (B) 2:1 PHYLLOSILICATE STRUCTURES, after Brindley and Brown (1980).

ORIGIN OF LAYER CHARGE IN 2:1 STRUCTURES

The 2:1 clay mineral structures may carry a permanent *layer charge,* or they may be electrically neutral. Permanent layer charge is the net negative charge per formula unit which occurs on 2:1 layers when the total charge of the anions in the structure exceeds the total charge of the cations. Layer charge may arise from isomorphic substitution, structural imperfections, broken bonds at the edges of particles, and exposed structural hydroxyls. All sources of layer charge are pH dependent with the exception of isomorphic substitution which is independent of pH. Isomorphic substitution is cited by van Olphen (1977) as the primary source of charge deficiency in 2:1 clays and may arise from any combination of the following four mechanisms (Guven, 1988):

(1) substitution of R^{3+} or R^{2+} for Si^{4+} in the tetrahedral sheet,

(2) substitution of R^{1+} or R^{2+} for R^{2+} or R^{3+}, respectively, in the octahedral sheet,

(3) presence of octahedral vacancies,

(4) dehydroxylization of OH to O

Layer charge may originate in the tetrahedral and/or the octahedral sheet, but the charge originating in one component sheet may be off set by an opposite charge in the other component sheet. Despite its origin, the layer charge is neutralized so that the crystal as a whole is electrically neutral. Electroneutrality is accommodated by the intercalation of *counter* or *interlayer ions* into the *inter-lamellar* or *interlayer* space between clay layers.

NATURE OF THE INTERLAYER

The interlayer is the space between 1:1 or 2:1 layer packets, and the composite of a layer and interlayer is termed the *unit structure*. Various interlayer complexes may occupy the interlayer region including cations, hydrated cations, organic cations, cations solvated with either polar or nonpolar solvents, and macromolecules, i.e., large organic cations. The number of cations occupying the interlayer position is assumed to be stoichiometric with respect to the net negative layer charge (Guven, 1988). Univalent and divalent cations are common counter ions with higher valency cations less common as interlayer complexes.

Two favorable positions for cations without hydration shells occur in 2:1 structures with R^{3+} tetrahedral substitution. The first is in the interlayer at the center of an oxygen triad with excess charge and coincident with the tetrahedral R^{3+} cation. The second is partially within the hexagonal cavity of the tetrahedral sheet and closer to the two basal and one apical oxygen of a tetrahedra with R^{3+} substitution. In the latter case, univalent cations of the proper size can penetrate into the hexagonal cavities of the teterahedral sheet and bond to one smectite layer. Larger univalent cations, such as potassium, move to a position above the hexagonal cavity and bond with two oxygens from adjacent layers,

thereby, creating a cohesive force between layers. If the chemical and/or thermal regimes are appropriate potassium ions may form permanent bonds in the interlayer of smectites and the formation of illitic layers may result. Interstratification of illite and smectite represents an intermediate phase between pure smectite and pure illite. I/S may either be regular, i.e., a definite ordering of the two component layers, or random with no systematic variation of the component layers.

The most favorable interlayer position for divalent cations is at the center of an oxygen triad with excess charge. An alternate but less stable position, is within the hexagonal cavity, bonding with two charged oxygens from each adjacent layer.

HYDRATION AND EXPANSION OF SMECTITES

To understand the adsorption of hydrophobic substances on hydrophillic surfaces (clay surface) it is helpful to examine the hydration characteristics of smectites. Hydration is dependent upon the solvation characteristics of the interlayer cation, and the magnitude and location of the negative charge within the crystal structure. Water adsorbed by smectites can be found in two states, either solvating the exchangeable cations, or in the "free" state about the external regions of the clay platelets (Sposito and Prost, 1982). The latter is favored at high water contents and the former at low water contents. Sposito and Prost (1982) have proposed that the location of the charge deficit within the smectite structure determines the spatial arrangement of water molecules solvating the interlayer cations. If octahedral substitution is responsible, the charge deficit on the surface oxygens is delocalized and adsorbed water molecules form only weak hydrogen bonds with the surface atoms (Fig. 1-7a). On the other hand, if the negative charge arises from tetrahedral substitution, the excess charge is

more localized, and formation of strong hydrogen bonds between the adsorbed water and the basal oxygens near sites of substitution is favored (Fig. 1–7b).
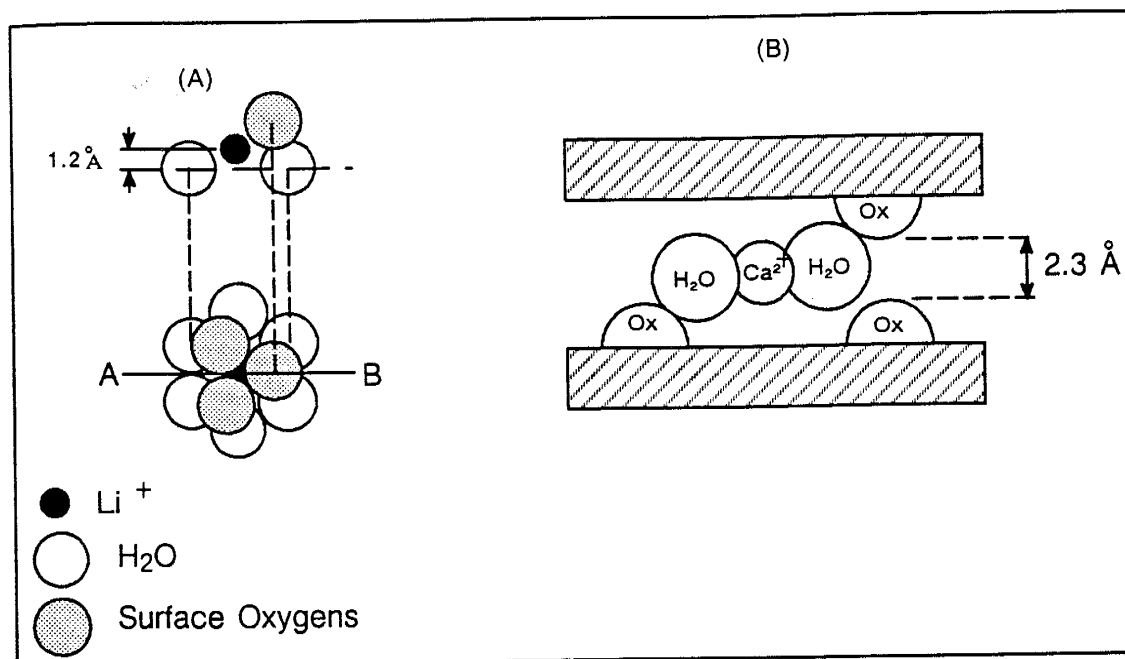
Fig. 1–7. Spatial arrangement of water molecules solvating (A) exchangeable Li+ on hectorite with octahedral substitution, in plan and section view in the A–B plane, (B) exchangeable Ca+ on smectite (saponite) with tetrahedral substitution, section view (after Sposito and Prost, 1982).

Based on infrared spectroscopic studies, Sposito and Prost (1982) have described a hydration mechanism for smectites. The first stage of hydration depends upon the initial interlamellar space, and the ability of water molecules to enter the structure. Initially, water entering the interlayer position solvates the counter ion, which for univalent ions is three water molecules and for divalent ions is more.

During the first stage of hydration, cations which were occupying the hexagonal cavities in the tetrahedral sheets may now move to a position midway between adjacent silicate layers. In the second stage as hydration continues, octahedral solvation complexes form about univalent cations, and second hydration sheaths form about divalent cations. The extent of hydration at this stage is de-

termined by the solvation strength of the cation, and thus, up to four mono-layers of adsorbed water may result, with basal spacings of approximately 19 $\overset{\circ}{A}$ (Barshad, 1950). However, formation of a complete monolayer of adsorbed water on the clay surface might not occur. Prost (1975) has demonstrated that the fraction of interlayer space covered by water molecules at given water content strongly depends on the solvation energy of the cation. Beyond the hydration of the exchangeable cations, the water adsorbed by smectites can condense in micropores and on external surfaces of the crystal structure (Sposito and Prost, 1982).

Expansion is the physical manifestation of adsorption of water or other substances into the interlamellar areas of an expanding lattice clay mineral, or for non-expanding phyllosilicates, between 1:1 or 2:1 layers. Expansion begins with the hydration of the interlayer cations at short particle distances and continues until a diffuse double layer of ions forms about the clay particle at the point of complete dispersion (van Olphen, 1977). The two types of swelling described are crystalline and osmotic, respectively. The former being dominant at short particle ranges and the latter at long particle distances. Only short-range expansion phenomena will be discussed here because it pertains, specifically, to the physical behavior of stratified clay-dominated systems.

Three forces contribute to expansion of the smectite crystal structure: 1) van der Waals interactions between layers, 2) electrostatic interaction between layers, and 3) the hydration energy of the interlayer cation (van Olphen, 1977). The contribution of electrostatic interaction depends upon the charge density of the clay surface and the position of the interlayer cation during hydration (Sposito and Prost, 1982). If the interlayer cations move to points midway between clay layers during hydration, the electrostatic interaction between layers is

an attraction. In this case the attractive force between layers will be great, and the hydration energy should also be high; that is, equal to the electrostatic attraction plus the van der Waals attraction. The driving mechanism of expansion is than the extent of hydrolysis of the interlayer cation in the confined space of the interlayer region.

Norrish (1954) has shown that the intracrystalline expansion of smectites is a function of the radius and valency of the interlayer cation. Norrish states that the attractive force between layers is greater when the interlayer cation is divalent as opposed to monovalent. Therefore, the energy of hydration of the interlayer cation must be greater than the work required to overcome the attraction between the cation and the negatively charged silicate layers. Since the work necessary to expand a crystal structure with divalent interlayer cations is greater than if the cations were monovalent complete hydration of divalent cations does not occur and the result is a lesser degree of expansion. By holding the surface charge density and the interlayer cation constant Norrish defines the index of swelling as the ratio of the repulsive to attractive forces between silicate layers as:

$$Index \ of \ swelling \ = \ \frac{U \times \epsilon}{v^2}$$

where,

U = Total hydration energy of a particular cation

v = Valence state of the cation

ϵ = Dielectric constant of the interlayer media

It is apparent from the definition that the swelling potential depends on the dielectric constant of the interlayer medium. Holding the other variables constant

(interlayer cation and surface charge density) and increasing the dielectric constant (relative permittivity) of the interlayer dielectric should result in expansion of the structure in the c-direction.

In Norrish's definition of swelling potential, only the properties of the interlayer cation and interlayer dielectric are considered and the properties of the surface are neglected. Keeping the interlayer dielectric and cation constant and varying the surface charge density should result in large attractive forces at high-charge densities, and low-attractive forces at low-charge densities. Therefore, the work required to expand high-charge smectites is greater than the work required for low-charge smectites, and low-charge smectites are expected to swell to greater extent.

The physical changes in the lattice of expanding 2:1 layer silicates which occurs upon expansion have been studied using X-ray diffraction techniques and are summarized as follows: the c-dimension of a particular smectite increases as a linear function of the moisture content (Ravina and Low, 1972). This phenomenon can be explained in terms of the adsorption of successive layers of water molecules in the interlayer space up to a limiting value which is determined by the transition between short- and long-range particle interactions (approximately 19 $\overset{\circ}{A}$). At the transition maximum, interactions of composite clay packets is minimalized and the clay plates tend to behave individually with edge-face interactions (i.e., positively charged crystal edges attracted to negatively charged crystal faces), and the formation of a diffuse double layer of ions about the plates determining the properties of the medium.

Ravina and Low (1972) have shown that the b-crystallographic dimension of dioctahedral sodium smectite may also change as a function of moisture content. As the moisture content increased the b-dimension of the crystal in-

creased continuously to a maximum value of approximately 9.0 Å which was constant for all smectites they examined regardless of their cation exchange capacity. Ravina and Low attribute this change in the b-direction to an alteration of bond angles and/or bond lengths by external forces. Similar forces which contribute to expansion in the c-crystallograghic direction may also be responsible for alterations in the b-direction. The implication of Ravina and Low's study is that alteration in the c-direction accompanied by a simultaneous change in the b-direction for smectite-water interactions may also occur in smectite-organic interactions.

CLAY-ORGANIC INTERACTIONS

GENERAL

The study of clay-organic reactions has received a great deal of inquiry in a variety of fields ranging from ceramics to petroleum recovery. Adsorption of organic compounds is not limited to the exterior surfaces of clays but may also occur in the interlamellar spaces between 1:1 and 2:1 layers; this is particularly important for the expandable lattice clay minerals, smectite and vermiculite, which have permanent charge deficiencies. Thus, the formation of *clay-organic complexes* in the interlayer region of expanding lattice clays are of primary interest in the study of clay-organic reactions.

ADSORPTION FORCES AND MECHANISMS

Adsorption of hydrophobic organic compounds at the liquid-solid interface is a complex and imperfectly understood process which in recent years has met with considerable controversy (Chiou, 1979; Mingelgrin et al., 1983). The following adsorption mechanisms are summarized from Griffin and Roy (1985),

and only pertain to compounds which are not ionized or strongly polar when present in an aqueous environment.

1) *van der Waals*. These are attractive forces which arise from momentary dipoles about atoms or molecules caused by small perturbations of the electron motions. These dipoles induce small dipoles of opposite sign in neighboring atoms. Although the momentary and induced dipoles are dynamic in position and sign, the net result is a weak attractive force. These forces could be important in the adsorption of compounds which are either weakly polar (TCE and xylene), or nonpolar (tetrachloroethene (PCE) and benzene).

2) *Hydrogen bonding*. In this interaction a hydrogen atom is bonded to two or more other atoms. The "bonds" are generally conceived as an induced dipole phenomena. There is no universal agreement on the best description of the hydrogen bond (Huheey, 1978), but it may be considered as the asymmetric electronic distribution of the *Is* electron of the hydrogen atom by highly electronegative atoms, such as F, O, Cl, and S. Hydrogen bonding is one of the mechanisms of smectite hydration, where bonds form between the basal oxygens of the tetrahedral sheet and the hydrogen atoms of the sorbing water molecules. The adsorption of halogenated organics such as TCE, PCE, and carbon tetrachloride (CCl_4) in the interlayer of smectites may also be explained by hydrogen bonding, by which the highly electronegative halogen atom of the organic compound bonds with the hydrogen atoms of the interlayer water.

3) *Dipole–dipole* or *orientation energy*. This force results from the attraction of molecules with permanent dipoles. These forces may be responsible for the adsorption of compounds, such as acetone which could replace the water of hydration at the interlayer.

4) *Induction* or *dipole induced dipole*. This results from the attraction of an induced dipole brought about by either a permanent dipole or a charged site or species. These type of interactions may be an important mechanism for adsorption of organics with small dipole moments, such as xylene and toluene.

5) *Hydrophobic effect*. The adsorption forces described thus far are all forms of weak electrostatic bonds, and in a given system any number of them may be contributing to the adsorption process. However, for neutral nonpolar organic compounds which do not exist in aqueous solution as ionized species the degree of electrostatic interactions is minimal, and other modes of adsorption are at work.

Hydrophobic compounds are substances which are readily soluble in nonpolar organic solvents, but are only sparingly soluble in water. The low aqueous solubility is due to the lack of electrostatic attraction between the nonpolar organic molecule and the dipolar water molecule. The lack of interaction causes hydrophobic compounds to minimize contact with the aqueous environment and seek relatively nonpolar environments. The former statements form the basis for hydrophobic bonding theory.

The hydrophobic theory has been widely applied to adsorption of hydrophobic compounds in soil environments. Two schools of thought exist concern-

ing the process of removing hydrophobic solutes from solution: 1) partition theory, and 2) the adsorption theory.

The partition theory supports the idea that nonpolar organic solutes escape the polar aqueous environment by dissolving or partitioning into the organic fraction of the soil. The nonpolar "solvent" of the soil environment is the organic matter derived from the degradation of plant and animal matter. It is believed that hydrophobic pollutants occurring either in an aqueous phase or as a pure organic phase "partition" into the soil organic fraction, and thus, attenuation of these pollutants by the soil is a function of the amount of organic matter present in the soil (Chiou, 1979).

The work of Mingelgrin et al. (1983), however, disputes the previous author and presents data which confirms that geologic materials (clays) with the organic matter removed still attenuate hydrophobic compounds. The adsorption theory is based on the theory that hydrophobic "escape" from a polar environment is thermodynamically favorable due to large positive increases in the entropy of the system. Due to the lack of electrostatic interaction of a nonpolar organic solute with water the organic's presence in an aqueous environment tends to decrease the free volume of water (Griffin and Roy, 1985). The organic is surrounded by a shell of water molecules having some type of quasi–structure ordered by van der–Waals forces between the the solute and water molecules. The entropy increase arises from the destruction of these highly ordered water structures around the hydrophobic compound upon adsorption to the mineral surface (Griffin and Roy, 1985).

The adsorption theory of hydrophobic removal from the aqueous environment is probably the mechanism responsible for the formation of clay–organic complexes. If this is the case, the work associated with expanding or contract-

ing the crystal structure must be less than or equal to the energy liberated from the removal of the hydrophobic compound from solution (entropy increase) for the free energy of the system to be negative, and hence, spontaneous interlayer adsorption to occur.

INTRACRYSTALLINE SWELLING BY ORGANIC COMPOUNDS

The swelling of montmorillonite in organic liquids of varying properties has received considerable attention (Barshad, 1952; Norrish, 1954; Brindley et al., 1969; Olejnik et al., 1974; Berkheiser and Mortland, 1975; Brindley, 1980). These previous studies suggest that some relationship exists between the dielectric constant of the organic compound and the c-axis dimension of the clay-organic complex. They also point out that the dipole moment of the organic may also have an effect on the final c-axis dimension of the clay-organic complex. Griffin and Roy (1983) also suggest that the molecular weight of a compound may have an affect on the final c-axis dimension of clay-organic complexes.

The dielectric constant or relative permittivity of a solvent is defined as the measure of the relative effect the solvent has on the force with which two oppositely charged plates attract each other (Riddick and Bunger, 1970). The dielectric constant is a unitless value which, in a vacuum, is defined as unity. Therefore, solvents with large dielectric constants tend to decrease the force of attraction between two oppositely charged plates.

The effect of replacing an interlayer solvent of high dielectric constant (water) with one of low dielectric constant (nonpolar organic) should be an increased electrostatic attraction between the interlayer cation and the negatively charged silicate layers resulting in a decrease of the c-axis dimension of the clay structure. The literature (Barshad, 1952; Norrish, 1954; Brindley et al.,

1969; Olejnik et al., 1974; Berkheiser and Mortland, 1975; Brindley, 1980) supports these conclusions, but the relationship between dielectric constant and c-axis dimension is nonlinear and other factors such as dipole moment may come into play.

The dipole moment is a measure of the displacement of the center of positive and negative charge on a molecule. It is the product of a charge and a distance and is expressed in units of either 10^{-18} esu or in Debye units, where $1D = 10^{-18}$ esu.

Two factors affect the magnitude of the dipole moment, 1) the symmetry of the molecule, and 2) the presence of highly electronegative elements such as O, F, Cl, and Br. Symmetric molecules are nonpolar, i.e., their dipole moment is equal to zero. Non-symmetric molecules tend to be polar, particularly those with highly electronegative elements. An example of a nonpolar organic molecule with highly electronegative group is carbon tetrachloride. The perfect symmetry of the CCl_4 molecule renders it nonpolar.

The effect of polarity on adsorption is that polar compounds are preferentially adsorbed over nonpolar compounds at charged sites. This makes good sense in light of the fact that with the exception of hydrophobic bonding, all other adsorption mechanisms considered here are forms of electrostatic interactions.

While polar compounds are preferentially adsorbed over nonpolar compounds, the relationship between dipole moment and the c-axis dimension of clay-organic complexes is not as clear cut. Barshad (1952), showed that expansion of smectite in solvents of similar dielectric constant and increasing dipole moment can cause either an increase or a decrease in the c-axis dimension.

Barshad attributes this inconsistency to the stronger association of a solvent with high dipole moment for itself which results in the closer packing of the solvent molecules in the interlayer region, and hence, a decrease in the c-direction. On the other hand, Barshad showed that a Ca-smectite was expanded by a solvent, acetone, with higher dipole moment, relative to n-butanol, both of which have similar dielectric constants. This could possibly be explained by acetone having a lower molecular weight than n-butanol and allowing for more acetone to be adsorbed (Griffin and Roy, 1983), and thus a greater c-axis dimension.

The effect on intracrystalline swelling of two compounds with similar dipole moments but different molecular weights is that the compound with higher molecular weight will form a clay-organic complex with a smaller c-axis dimension than the low molecular compound. Although high molecular weight compounds are preferentially adsorbed over low molecular weight compounds high molecular weight compounds can not form as many adsorbed fluid layers on the mineral surface (Griffin and Roy, 1983), and thus the c-axis dimension of a high molecular weight clay-organic complex will be less than a low molecular weight clay-organic complex. This phenomena can be viewed in terms of the charge density on the molecule, e.g., for two compounds with similar dipole moments the low molecular weight compound will have a more localized (greater) charge density than the higher molecular compound which results in a greater number of the low molecular weight molecules being adsorbed per charged adsorption site.

Although not discussed in the literature as being an organic property to which any correlation has been made to organic-inorganic reactions the log of the n-octanol-water partition coefficient (log K_{ow}) and the final c-axis dimension of clay organic complexes may be related. The K_{ow} is the ratio of the con-

centration of a substance dissolved in n–octanol to that dissolved in water. For hydrophobic compounds this value is large and for hydrophillic compounds it is small. Values of K_{ow} range over several orders of magnitude therefore, making the log K_{ow} a more manageable value.

The octanol–water system is believed to imitate bioaccumulation in living tissues, and has been applied to the adsorption of organic compounds in soil environments based the percent organic matter present in the soil (Kenaga and Goring, 1980). Karickhoff (1979) defined a relationship between the soil adsorption coefficient (Freundlich adsorption coefficient divided by the organic carbon fraction or K_{oc}; see Griffin and Roy (1985) for discussion of K_{oc}) and the log K_{ow} as given by:

$$\log \ K_{oc} \ = \ \log \ K_{ow} \ - \ 0.21$$

Hansch et al. (1968) found a linear relationship between the aqueous solubility of organic compounds and their octanol–water partition coefficient. The octanol–water partition coefficient may be an indication of the hydration energy of the solvent–water system.

Other factors influencing crystalline expansion are the interlayer cation, the total layer charge of the crystal, and the initial c-axis dimension prior to organic immersion. Only the latter will be discussed as the former two factors were covered in the section on hydration and expansion.

The initial c-axis dimension of an expanding lattice clay mineral prior to organic saturation is determined by the interlayer cation and its degree of hydration. Several investigators (Barshad, 1952; Norrish, 1954; Olejnik et al., 1974; Berkheiser and Mortland, 1975) completely dehydrate their samples by heating

at 250°C prior to organic saturation which results in a collapse of the smectite structure to approximately 10 $\overset{\circ}{\text{A}}$ in the c–direction. By removing the interlayer dielectric (water) and replacing it with a dielectric of considerably lower relative permittivity (air) the attractive force of the silicate layers for the interlayer cation is substantially increased. The relationship between the attractive force and the dielectric constant is given by:

$$E = \frac{\sigma\ v\ e}{2\ D\ \epsilon}$$

where,

E = attractive force

σ = the surface charge density

v = the valency of the interlayer cation

e = the elementary charge

D = the distance between the cation and the surface

ϵ = dielectric constant of the interlayer medium

(Norrish, 1954)

Due to the increased attractive force between silicate layers the energy of hydration must be great enough to overcome the work required to expand the collapsed crystal structure. Since cations do not to hydrate with compounds of low dielectric constant (e.g., nonpolar organics) the probability of opening up a collapsed lattice with a low dielectric media is decreased. Hence, the greater the initial c–axis dimension the greater is the propensity for the expansion and contraction of the crystal structure.

In summary, the potential of swelling for an expandable lattice clay is a function of the properties of the interlayer surface, the interlayer cation, and the medium separating the silicate layers.

ORGANIC EFFECTS ON INTERPARTICLE DISTANCES OF NON–SWELLING CLAYS

Murray and Quirk (1982) and Green et al. (1983) studied the physical swelling, i.e. non–crystalline swelling, of non–expanding clay minerals in organic solvents using consolidation theory. The consolidation apparatus allows for slight volume changes in the sample material to be measured while the pore fluid of the sample is changed. The results of these studies revealed that the physical swelling of these clays was less when saturated with organic compounds than with water.

Murray and Quirk (1982) found a linear correlation between the dielectric constant of the saturating fluid and the physical swelling of the soil. Murray and Quirk (1982) proposed mechanisms similar to those which effect the intracrystalline swelling of smectites as responsible for the phenomena observed with illitic material of their study.

The study of Green et al. (1983) revealed a negative non–linear correlation between the bulk swelling of the clays and the log K_{ow} of the solvents. They explained the negative correlation in terms of solvents with small or negative log K_{ow}'s being more soluble in the pore water between clay platelets and thus causing the clay to swell by the same physical mechanisms which cause intracrystalline swelling of smectites.

2.3 ORGANIC EFFECTS ON SATURATED HYDRAULIC CONDUCTIVITY

In the previous section it was shown that organic chemicals can change the c-axis dimension of expanding-lattice clay minerals and the interparticle distances of non-expanding clay minerals. Thus, it comes as no surprise that organic chemicals may also alter the hydraulic conductivity of clay systems by changing the pore dimensions and geometries of the porous medium. A great deal of literature dealing with the integrity of clay waste disposal liners indicate that hydraulic conductivity of these materials is commonly measured using 0.01N $CaSO_4$ or $CaCl_2$ solutions (Acar et al., 1985; Anderson and Brown, 1981; and Parker et al., 1984). Use of dilute water to measure hydraulic conductivities fails to predict the materials reaction to solutions of variable chemical properties, eg., leachate generated at a disposal site or a hydrocarbon spill on the land surface. If a clay material is slated for use as a liner material or if a clay-rich geologic horizon is a suspected "impermeable" barrier to the transport of organic contaminants to the groundwater then tests should be performed to determine the clay's tolerance to a variable chemical environment.

Previous studies by Acar et al. (1985), Anderson and Brown (1981), Green et al. (1981), Parker et al. (1984), and Schramm et al. (1986), reveal that organic chemicals of varying properties affect clay dominated systems in a similar manner by increasing their hydraulic conductivities relative to water. Discrepancies exist in comparing the results of these researchers due to the variability in their experimental apparatus (flexible vs rigid wall permeameters; consolidation cell, and compaction mold permeameters), the experimental procedures followed by each (initial wetting fluid and the hydraulic gradients imposed on the system), and the materials they used (dominant clay mineral phase present in the porous media).

Acar et al. (1985) compared the results of the effect of acetone on a compacted kaolinite in flexible wall vs rigid wall permeameters. The comparison showed that the rigid wall permeameter yielded hydraulic conductivities two orders of magnitude greater than that for the flexible wall permeameter packed with the same material. Acar et al. (1985) attributed the increased hydraulic conductivity to shrinkage of the clay in the acetone and flow along the walls of the permeameter thus giving values too high. Similar to the rigid wall permeameter, the compaction mold apparatus used by Anderson and Brown (1981) did not compensate for volume changes of the sample and flow along the walls may occur if the sample shrinks during testing. The consolidation cell apparatus used by Parker et al. (1984) automatically compensates for volume changes by adjustment of the consolidation stress. Regardless of the apparatus employed to determine the hydraulic conductivity of fine-grained materials, as long as careful experimental technique is exercised the researcher should be able to observe when flow is occurring along the walls of a column.

The initial wetting fluid of the clay material in association with the hydraulic gradients imposed on the column affects the ability of the nonaqueous phase to flow through the column. In the studies of Parker et al. (1984) and Schramm et al. (1986), the dry clay material was initially wetted with organic compounds. The results of these studies indicate that the flow of an immiscible organic compound (xylene) through the clay material caused the hydraulic conductivity to increase relative to that measured with water (0.01N $CaCl_2$ aqueous solution).

While Parker et al. (1984) and Schramm et al. (1986) found an increase relative to water for an immiscible organic, Acar et al. (1985) Anderson and Brown (1981) and Green et al. (1981) found that immiscible organic compounds

decreased the hydraulic conductivity of the clay materials relative to water. This discrepancy is explained by the fact that Acar et al. (1985), Anderson and Brown (1981), and Green et al. (1981) initially wetted their samples with water and not the organic compound, a much more realistic situation.

With the samples initially water–wet, the saturating organic compound must initially displace the water from the pore spaces before acting upon the physical properties of the clay. Water is the wetting phase in the clay–water–organic system (i.e., its contact angle with the clay surface is less than 90°), and the organic is the non–wetting phase. If the example of air displacing water in a capillary tube is an analogy to an immiscible organic displacing water in a pore space, then the definition the displacement pressure is the same as the capillary pressure (P_c), Fig. 1–8.

$$P_c = \frac{4\sigma \cos\theta}{D}$$

where,

θ is the contact angle between the fluids.

σ is the interfacial tension between the fluids.

D is the pore diameter.
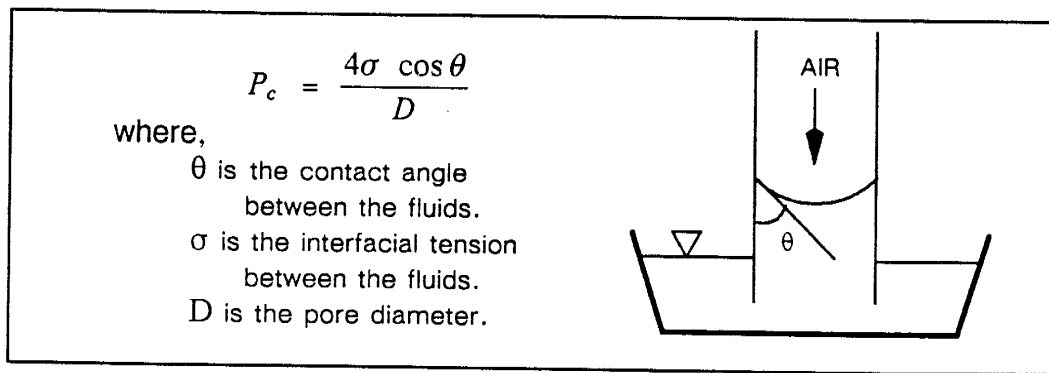
Figure 1–8. EQUATION OF CAPILLARY PRESSURE, from Bear (1972).

Therefore, to replace a wetting phase with a non–wetting phase the capillary pressure must be equaled or exceeded. From its definition the capillary pressure will increase as the contact angle and pore diameter decreases, and the interfacial tension increases.

Based on the prior discussion it becomes clear why the hydraulic conductivity apparently decreases with immiscible organics relative to water. However,

should the critical capillary pressure be exceeded for the immiscible phase and immiscible displacement occur then it can be expected that alteration of the hydraulic conductivity will occur as dictated by the specific clay–organic interaction.

Acar et al. (1985) demonstrated that benzene and chlorobenzene at low hydraulic gradients cause a decrease in the hydraulic conductivity of a compacted kaolinite relative to water. When the hydraulic gradient was increased and exceeded the critical capillary pressure of displacement, the hydraulic conductivity increased to a value greater than that for water. Similarly, for organic chemicals which are miscible in water or have a high aqueous solubility (e.g., acetone, methanol, and aniline), the prior investigations (Acar et al., 1985; Anderson and Brown, 1981; Green et al., 1981; Parker et al., 1984; and Schramm et al., 1986) indicate that the hydraulic conductivity of clay materials always increases in their presence.

Since clays in the natural environment are normally water–wet and since natural hydraulic gradients are rarely as high as those in the laboratory, it seems unlikely that the critical capillary pressure would ever be achieved for immiscible displacement to occur in a clay system. However, in areas of known contamination, it is common for a variety chemicals to make up the contaminated fluid. If the contaminated fluid is a composite of miscible and immiscible phases, then cosolvent effects may allow for the passage of the immiscible phases into the clay i.e., the miscible phases may increase the solubility of the immiscible phases which could result in a decrease in the c–axis dimension of the clays and increase the hydraulic conductivity of the layer.

CHAPTER 2

MATERIALS AND METHODS

2.1 MATERIALS

Seven discontinuous split spoon cores from the SJ–6 site were obtained from the New Mexico Environmental Improvement Division. Each was examined to determine the interval most representative of the shallow aquitard material. Based on clay content and its occurrence in 5 of the 7 SV cores obtained from the NMEID, the material in the interval of 2.0–4.0 meters from core SV–15 was chosen as the experimental medium. In addition to materials from the site, a reference clay, STx–1 montmorillonite, was selected for use in the intracrystalline expansion phase of the study. The reference clay was obtained from the Source Clays Repository at the University of Missouri, Columbia.

The standard "water" used in this study is composed of calcium chloride ($CaCl_2$) dissolved in distilled water to a concentration of 300 ppm. This concentration was chosen because a preliminary study determined it to prevent dispersal of clay in the SV–15 material, and because it is typical of local groundwater at the SJ–6 site (Hart Associates Inc.). Several organic compounds were chosen for the study based on their occurrence at the SJ–6 Superfund site and other hazardous waste sites, and on the variability of their chemical properties

ORGANIC CHEMICAL PROPERTIES

The organic chemicals chosen can be divided into two groups: aromatic and aliphatic hydrocarbons, each of which can be further be divided into chlorinated and nonchlorinated compounds, and also, based on their dipole mo-

ment, into nonpolar and polar compounds. Table 2-1 lists all of the pertinent chemical information for each compound.

TABLE 2-1 *

ORGANIC CHEMICAL PROPERTIES

compound	aqueous solubility [1]	log K_{ow} [2]	dipole moment [3]	dielectric constant	formula weight	classification
water	——	-1.15	1.84	79.38	18.0153	——
benzene	0.178	2.13	0.00	2.28	78.115	aromatic hydrocarbon
toluene	0.0515	2.69	0.31	2.38	92.142	aromatic hydrocarbon
p-xylene	0.019	2.74	0.02	2.27	106.169	aromatic hydrocarbon
chloro-benzene	0.0488	2.77	1.54	5.62	112.560	chlorinated aromatic
methanol	infinite	0.66-0.83	2.87	32.70	32.042	aliphatic alcohol
acetone	infinite	-0.24	2.69	20.70	58.081	aliphatic ketone
dichloro-methane	1.30	1.40	1.14	9.10	84.933	aliphatic chlorinated
carbon tetrachloride	0.077	2.64	0.00	2.24	153.823	aliphatic chlorinated
trichloro-ethene	0.11	2.37	0.80	3.42	131.389	unsaturated chlorinated
tetrachloro-ethene	0.015	2.88	0.00	2.30	165.834	unsaturated chlorinated

* from: Riddick and Bunger (1970).
[1] aqueous solubility expressed as weight percent.
[2] log K_{ow} values from Griffin and Roy, 1985.
[3] dipole moment expressed in Debye units

GEOLOGIC MATERIAL PROPERTIES

Particle size, particle density, bulk mineralogy, and clay mineralogy were determined for the bulk SV-15 sample to be used in the remainder of the ex-

periments. These properties were determined using standard procedures which are described in Appendix A.

The properties of the bulk SV–15 material are as follows: particle size analysis, sand and larger 3.05 $\pm$0.3%, silt 37.4 $\pm$2.3%, clay 59.5 $\pm$2.4%. Bulk mineralogy, in order of relative abundance: clay minerals, quartz, feldspar, and calcite. Mineralogy of the <2μm fraction: Ca-smectite 3/10, I/S 3/10, illite 2/10, kaolinite 2/10, and quartz. Based on the diffuse nature of their diffraction maxima, the clay minerals are not well crystallized and are therefore interpreted as dominantly of detrital in origin.

A standard clay was chosen to compare results of the swelling experiments with that of the SV–15 clay. The STx–1 montmorillonite as described by Van Olphen and Fripiat (1979), is an Eocene bentonite from the Manning Formation of Gonzales County, Texas, and is a relatively pure bentonite with Ca-montmorillonite as the primary mineral phase present. It has a cation exchange capacity of 84.4 meq/100g, and calcium as the dominant exchangable ion.

3.2 EXPERIMENTAL METHODS

This study incorporated a microscale and macroscale approach to the investigation of how organic compounds effect the physical properties of clay minerals and clay dominated systems. On the microscale, X-ray diffraction methods were used to study the intracrystalline swelling properties of the <2μm fraction of the described materials in the presence of organic compounds. The organic chemicals chosen for this phase of the experiment are representative of those detected in soil and water analysis from the SJ–6 Superfund site and represent chemicals with varying properties (dipole moment, dielectric constant, and log K_{ow}). Closed cell permeameters were used in the macroscale study to inves-

tigate how the microscale clay–organic interactions affect a macroscopic property, hydraulic conductivity, of the clay–rich SV–15 geologic material. The permeants used in the column study were 300 ppm $CaCl_2$ aqueous solution to represent local groundwater and TCE, both in aqueous dilutions and in the pure phase, to represent the hydrophobic organic chemical.

INTRACRYSTALLINE PROCEDURES

The procedures used were similar to those used by Brindley et al. (1969). Samples of SV–15 and STx–1 were dispersed in deionized water and allowed to stand for 20 minutes. If the samples remained in suspension for 20 minutes, approximately 10 ml of the clay–water suspension was pipetted from just below the air–water interface and placed in a separate beaker. The original sample was then remixed and the procedure repeated until 50 ml of the <2μm fraction was separated.

Oriented clay slides were made using the filter peel technique of Drever (1973) (see Appendix A for procedure). No cation saturations were performed on the either SV–15 or STx–1 samples in order to preserve the original interlayer cation assemblages. The slides were dried and stored at room temperature (approximately 22°C), and ambient relative humidity (10–20%).

The air–dried slides were then sealed in glass solvation vessels with the organic compounds. Each of the sample slides was immersed in an organic liquid such that the liquid overlapped the clay film and permitted wetting of the clay by capillary action. Samples were allowed to equilibrate in the organic environment for one week prior to X–ray examination.

The sample slides were not dehydrated at elevated temperatures prior to immersion in the organic liquids. In previous studies (e.g., Barshad, 1952; Nor-

rish, 1954; Olejnik et al., 1974; Berkheiser and Mortland, 1975) investigators dehydrated their samples in order to determine if the organic compounds they used could initiate swelling of collapsed crystal structures. Since this study was concerned with the "field" condition of the clay minerals, and the effect organics have on clays which are naturally hydrated no attempt was made to dehydrate the clay minerals prior to organic immersion.

The solvated clay–organic slides were removed from the solvation vessels and sealed in SPEX mylar X-ray film for X-ray examination. The mylar film acted as a barrier to inhibit volatilization of the organic liquid from the surface of the sample during the X-ray procedure. A preliminary study determined that the mylar film did not cause dispersion of the X-rays or shifts in diffraction maxima.

Data were gathered from a Rigaku Dmax IA X-ray diffractometer using CuKα radiation set at 40 kV and 25 mA, a scan speed of 2°2θ/minute, and count rates ranging from 800 to 2000 counts full scale. Recordings were made of the 001 basal reflection of the primary clay phases present in the samples.

COLUMN PROCEDURES

Closed cell permeameters were designed after those used by Hagan (1989). Each permeameter consisted of a glass chromatographic column 2.5 cm in diameter, and 1.8 cm in length. The ends of the columns were threaded to accommodate teflon endcaps which had fixed stopcocks (Fig. 2–3). The columns were constructed of chemically resistant materials to prevent their degradation in the presence of volatile organic compounds.

Burets (100 ml) were used as supply vessels for the columns, and provided an accurate means of monitoring the volume of permeant passed through

the column. Vapor exchange vessels were constructed from Erlenmeyer flasks to impede volatilization of fluids from the buret head (Fig. 2-4). Two vapor exchange vessels were necessary to inhibit volatilization when running TCE solutions through the columns.
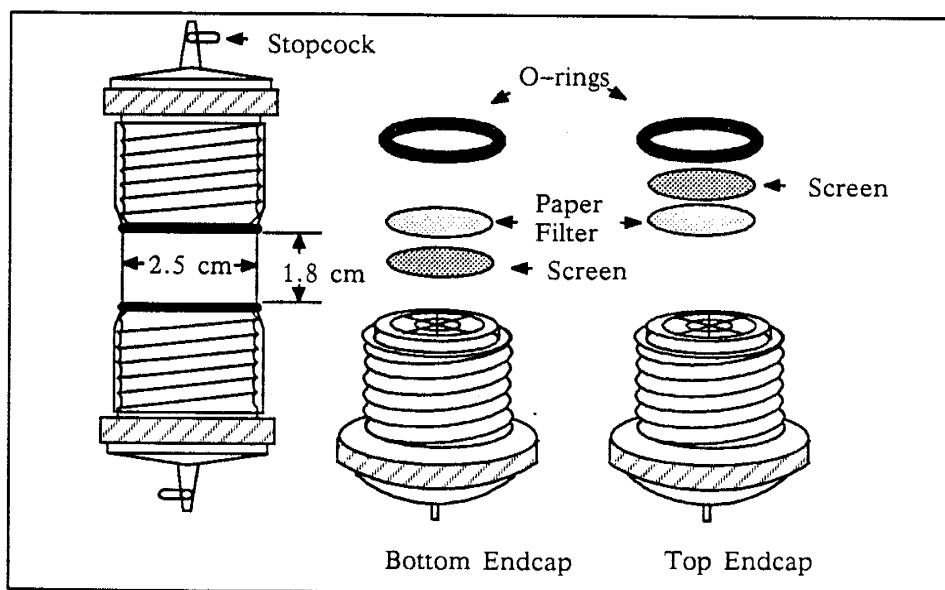
FIGURE 2-3. CLOSED CELL PERMEAMETER USED IN THE HYDRAULIC CONDUCTIVITY DETERMI-NATIONS, (After Hagan, 1989).

The bulk SV-15 clay material was crushed to a maximum particle size of 210 μm, and the sample split into three equal lots. Each of three columns were packed with the same bulk SV-15 clay material.

The columns were dry-packed using a funnel lifted in a circular motion off of the base of the column as the material poured out of the tip of the funnel. Settling was enhanced by tapping the sides of the column with a spatula until no further settling was observed, and additional material was added accordingly. After settling, a sample was slightly tamped with a flat-bottom plunger of appropriate diameter and the top endcap screwed into place. The endcap was tightened down to a predetermined mark which ensured a sample

length of 1.8 cm. The physical properties of each soil–column system (bulk density; porosity, and pore volume) are listed in Appendix A.

The packed columns were transferred to a preheated oven of 105°C for de-airing. The columns were allowed to heat for one hour with the stopcocks open to expel the majority of the interstitial air trapped in the pore spaces. De-aired columns were removed from the oven, stopcocks closed, and fixed in bench stands in an inverted position. The water inlet tubes were attached to the base (actually the column top) of the inverted columns, and the stopcock on the water supply buret and that on the column were opened (Fig. 2–4).
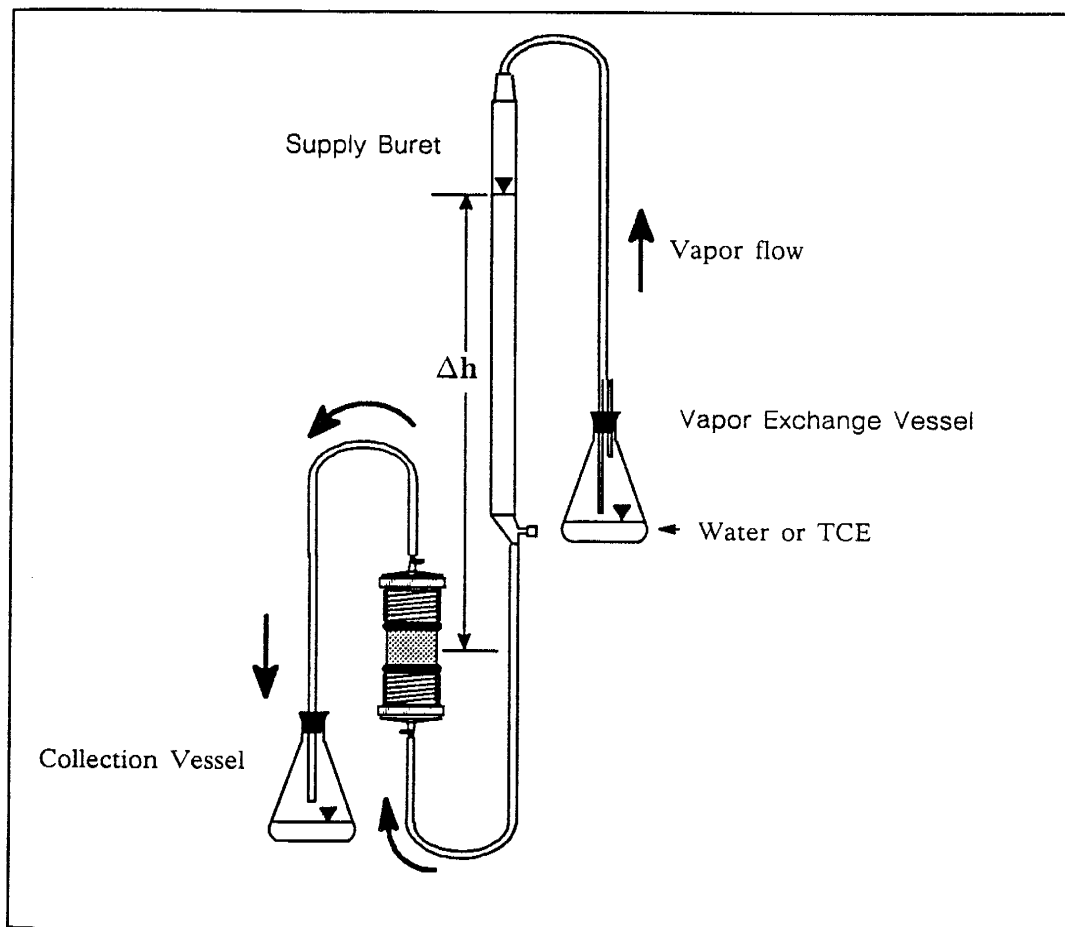
FIGURE 2-4. DIAGRAM OF COLUMN APPARATUS.

The vacuum formed in the cooling column formed a suction to draw water up into the column and speed the wetting process. Wetting from the bottom up insured a stable and uniform wetting front and prevented "fingering" or preferential flow, which may have led to air entrapment.

The de-airing technique described did not remove all of the interstitial air from the pores of the clay material and long stabilization times (2 weeks to one month) were necessary to completely de-air the columns. A column was deemed stable when no air bubbles formed at the column outlet and the hydraulic conductivity approached a constant value.

Column de-airing and baseline hydraulic conductivity values were obtained using the standard water. Upon stabilization, the permeant was changed to a solutions of TCE dissolved in standard water. Hydraulic conductivity measurements were made daily as the solution flowed through the column. The permeant concentration was increased every 20 pore volumes from an initial value of 250 ppm to 500 ppm to 1000 ppm, and finally to pure TCE.

The falling head method was used to evaluate the hydraulic conductivity of the SV-15 geologic material. This is a common means for determining hydraulic conductivity of fine-grained geologic materials and has advantage over the constant head method in that slight changes in head, i.e. slight flows are easily monitored (Olson and Daniel, 1981). The falling head equation is given by:

$$K = \frac{aL}{At} \ln \frac{h_1}{h_2}$$

where,

h_1 = initial head

h_2 = final head

t = time elapsed from h_1 to h_2

a = cross sectional area of supply buret

A = cross sectional area of sample

L = length of the sample

(Olson and Daniel, 1981)

CHAPTER 3

RESULTS AND DISCUSSION

3.0 RESULTS

The results of the intracrystalline expansion and the column studies were entered into computer files for ease of manipulation. Several Fortran 77 computer codes were either written or obtained to perform data reorganization, calculate statistical parameters, and to graphically display the data. The source codes for each of the programs used are listed in Appendix C.

INTRACRYSTALLINE EXPANSION RESULTS

The raw data from the intracrystalline study consisted of X–ray diffraction records from the SV–15 and STx–1 clays immersed in the organic liquids. The positions (degrees 2θ) of the diffraction maxima were recorded and converted to their corresponding d–spacing value by Bragg's Law:

$$d = \frac{\lambda}{2 \times \sin\theta}$$

d = d–spacing ($\overset{\circ}{A}$)

λ = wavelength of the incident radiation

(λ = 1.541838 for CuKα)

θ = position of the diffraction maxima (θ = degrees 2θ/2)

The results of the intracrystalline expansion study are compiled in table 3–1. Graphical display of the results for the chemical properties versus c–axis dimension are presented in this section with more detailed plots and interpretation of the data reserved for the discussion section to follow.

TABLE 3-1

Immersion Liquid	C-Axis Dimension (Å)		Organic Properties		
	SV-15	STx-1	log K_{ow}	dipole moment	dielectric constant
Benzene	13.29 ± 0.14	14.50 ± 0.33	2.13	0.00	2.28
Toluene	14.50 ± 0.33	15.25 ± 0.37	2.69	0.31	2.38
p-xylene	12.63 ± 0.05	15.24 ± 0.05	2.74	0.02	2.27
chloro-benzene	12.81 ± 0.05	15.11 ± 0.18	2.77	1.54	5.62
Methanol	12.81 ± 0.05	16.37 ± 0.05	0.66-0.83	2.87	32.70
Acetone	20.32 ± 0.33	17.67 ± 0.05	-0.24	2.69	20.70
Dichloro-methane	15.79 ± 0.05	14.26 ± 0.05	1.40	1.14	9.10
Carbon Tetra-chloride	12.46 ± 0.25	14.86 ± 0.18	2.64	0.00	2.24
Trichloro-ethene	13.40 ± 0.29	15.24 ± 0.05	2.37	0.80	3.42
Tetrachloro-ethene	13.39 ± 0.05	13.39 ± 0.05	2.88	0.00	2.30
300 ppm CaCl$_2$ H$_2$O	21.04 ± 0.05	19.64 ± 0.05	-1.15	1.84	79.38
1000 ppm TCE solution	21.10 ± 0.05	19.62 ± 0.05	——	——	——
500 ppm TCE solution	21.02 ± 0.05	19.64 ± 0.05	——	——	——
250 ppm TCE solution	21.04 ± 0.05	19.66 ± 0.05	——	——	——

TABLE 3-1. RESULTS OF THE INTRACRYSTALLINE EXPANSION STUDY.

The general trends of the dependency of c-axis dimension on the dielectric constant of the interlayer media are apparent in Figure 3-1. The dielectric constant increases as does the c-axis dimension of the clay-organic complex. The observed deviation from a linear relation is a reflection of other properties (e.g., dipole moment, molecular weight, and log K_{ow}) of the organic having a greater effect on the final c-axis dimension of the clay-organic complex than the dielectric constant.
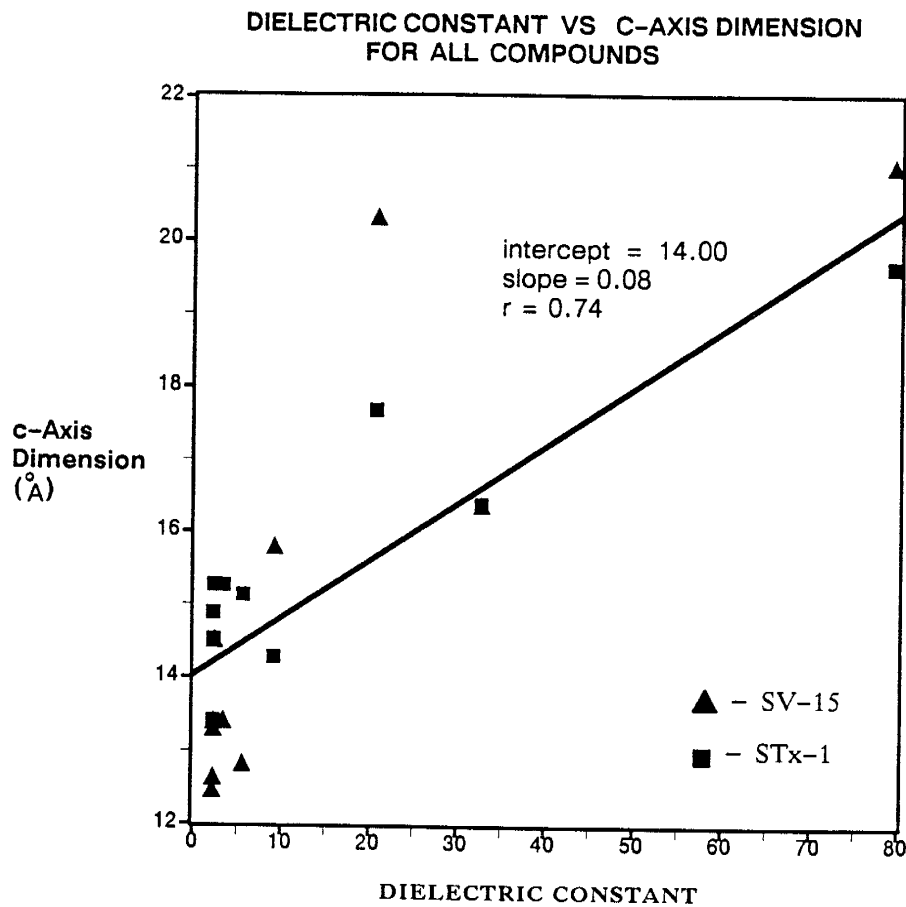
FIGURE 3-1. PLOT OF DIELECTRIC CONSTANT VS C-AXIS DIMENSION.

The results of the dipole moment of each organic compound plotted against the final c-axis dimension of the organic saturated clays are displayed in Figure 3-2 . A weak correlation exists between the magnitude of the dipole

moment and the extent of swelling (r = 0.55), but the scatter in the data suggests other mechanisms to be dominant in the control of the c–axis dimension. The poor correlation here strongly suggests that the dipole moment of a solvent has a minimal influence on the final c–axis dimension of its clay–organic complex.
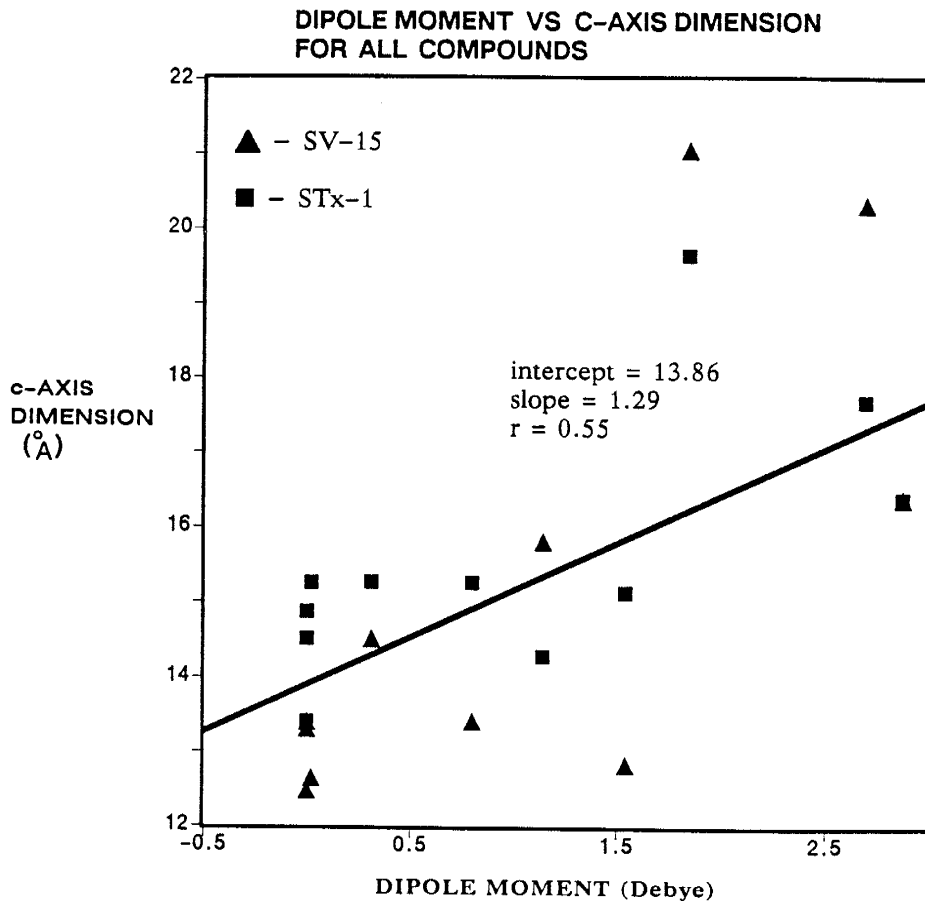
FIGURE 3-2. PLOT OF DIPOLE MOMENT VS C-AXIS DIMENSION.

Figure 3–3, displaying the data for log K_{ow} versus the c–axis dimension of the clay minerals, shows a strong inverse relationship of the final c–axis dimension of the saturated clays and the log K_{ow} of the organic compound. With the exception of some compounds with log K_{ow} values >2.0 the correlation (r= –0.83) to a straight line is high. This relationship may indicate a property of

the organic solvent which best describes the organics effect on the crystalline swelling of smectite clays.

LOG K_{ow} VS C-AXIS DIMENSION FOR ALL COMPOUNDS

intercept = 17.82
slope = -1.53
r = -0.83

▲ — SV-15

■ — STx-1
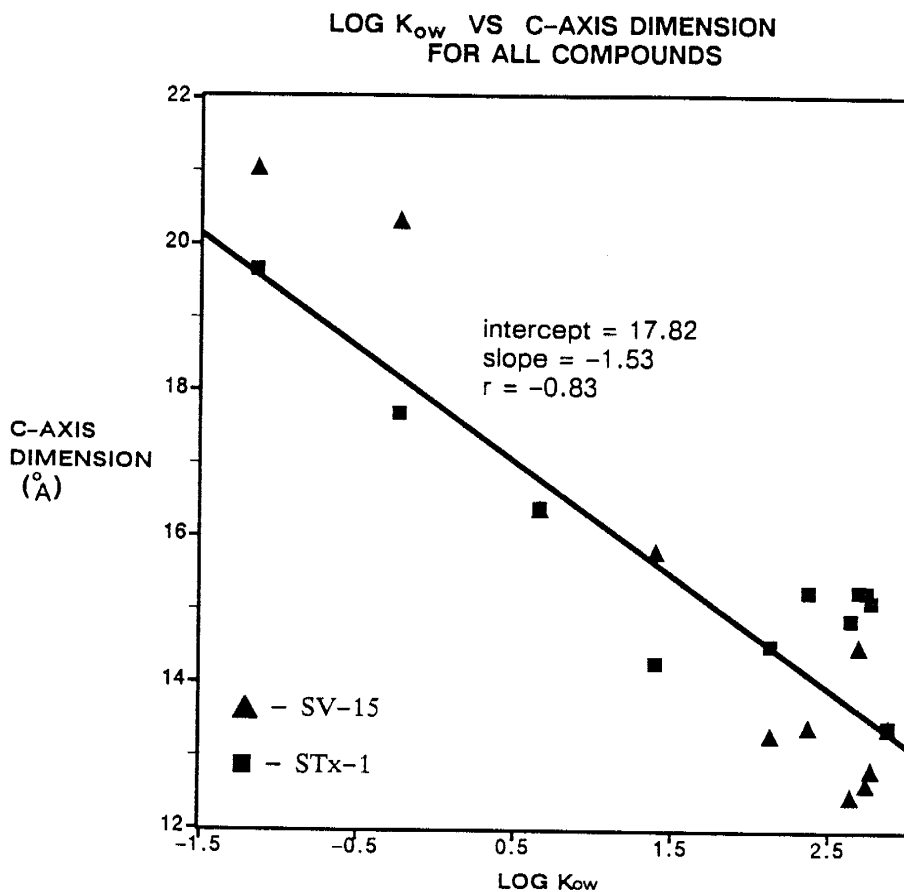
FIGURE 3-3. PLOT OF LOG K_{ow} VS C-AXIS DIMENSION.

The formation of clay-organic complexes with the non-swelling clay minerals of the SV-15 clay fraction occurred for some of the solvents. The presence of these complexes was recognized by the increased breadth the their respective 001 basal reflection as compared to their untreated air dried reflection. The increased breadth of the diffraction maxima indicates a less well-ordered structure, and hence, the formation of a clay organic complex. A relative measure of the crystallinity of a clay mineral may be obtained from its crystallinity index (Srodon and Eberl, 1984), which is the half height peak breadth of the

001 diffraction maxima (Kubler, 1964 as cited by Srodon and Eberl, 1984). Srodon and Eberl (1984) citing the work of Weaver (1960), observed that the 001 diffraction maxima of illite became sharper with increasing metamorphic and diagenetic grade indicating an increase in the crystallinity of the phase. It is assumed that as the crystallinity of a mineral phase increases its crystallinity index decreases. This same principle can be applied as a relative measure of clay-organic complex formation for non-expanding lattice clays. If clay-organic complexation occurs then the half height peak breadth of the 001 reflection will increase relative to the untreated 001 reflection. Table 3-2 lists the clay phases, organic chemicals, and the half height peak breadth of the clay-organic complex.

TABLE 3-2

CLAY	UNTREATED	ACETONE	DICHLORO-METHANE	TCE	PCE	CARBON TET.	CHLORO-BENZENE
ILLITE	2.5	5	BD	4.5	5.5	BD	4.5
KAOLINITE	2	2	BD	3	3	BD	2

TABLE 3-2. LISTING OF COMPOUNDS WHICH FORMED COMPLEXES WITH ILLITE AND KAOLINITE OF THE SV-15 CLAY, AND THEIR CRYSTALLINITY INDEX IN DEGREES 2θ. BD REFERS TO PEAKS WHICH WERE BROAD AND DIFFUSE, AND COULD NOT BE MEASURED WITH CONFIDENCE.

COLUMN STUDY RESULTS

Very little variation in the hydraulic conductivity values obtained for the different fluids was observed (Table 3-3). The standard deviation of the values from the population is greater for column B than for column A. Since the mean hydraulic conductivity of column B is less than that of column A by a factor of six, small errors in measurement and calculation of the hydraulic conductivity have a greater effect upon the standard deviation of column B than they do on the standard deviation of column A.

TABLE 3-3

column	300 ppm CaCl$_2$ water	250 ppm TCE	500 ppm TCE	1000 ppm TCE
A	6.50×10^{-7} $\pm 0.203 \times 10^{-7}$	6.56×10^{-7} $\pm 0.49 \times 10^{-7}$	6.50×10^{-7} $\pm 0.86 \times 10^{-7}$	5.70×10^{-7} $\pm 0.25 \times 10^{-7}$
B	1.08×10^{-7} $\pm 0.35 \times 10^{-7}$	1.03×10^{-7} $\pm 0.69 \times 10^{-7}$	0.99×10^{-7} $\pm 0.32 \times 10^{-7}$	0.99×10^{-7} $\pm 0.44 \times 10^{-7}$

TABLE 3-3. RESULTS OF THE COLUMN STUDY; MEAN HYDRAULIC CONDUCTIVITY FOR SOLUTIONS, in units of cm/sec.

Figure 3-4 displays the stabilization curves for columns A and B. The long stabilization times were to insure the removal of the entrapped air from the pore spaces to obtain accurate hydraulic conductivity measurements. The mean value of the hydraulic conductivity was calculated for each column using only the stabilized data.

The results of the TCE-saturated columns are presented graphically in Figure 3-5 with the mean values of hydraulic conductivity for the water saturated columns shown as dashed lines. It is obvious from this figure that the

TCE solutions had very little if any effect upon the hydraulic conductivity of the clay system.

The final saturation with pure TCE was unsuccessful for both columns. No TCE was able to pass through the columns at the hydraulic gradients imposed on the system, and as a result no macropores formed.
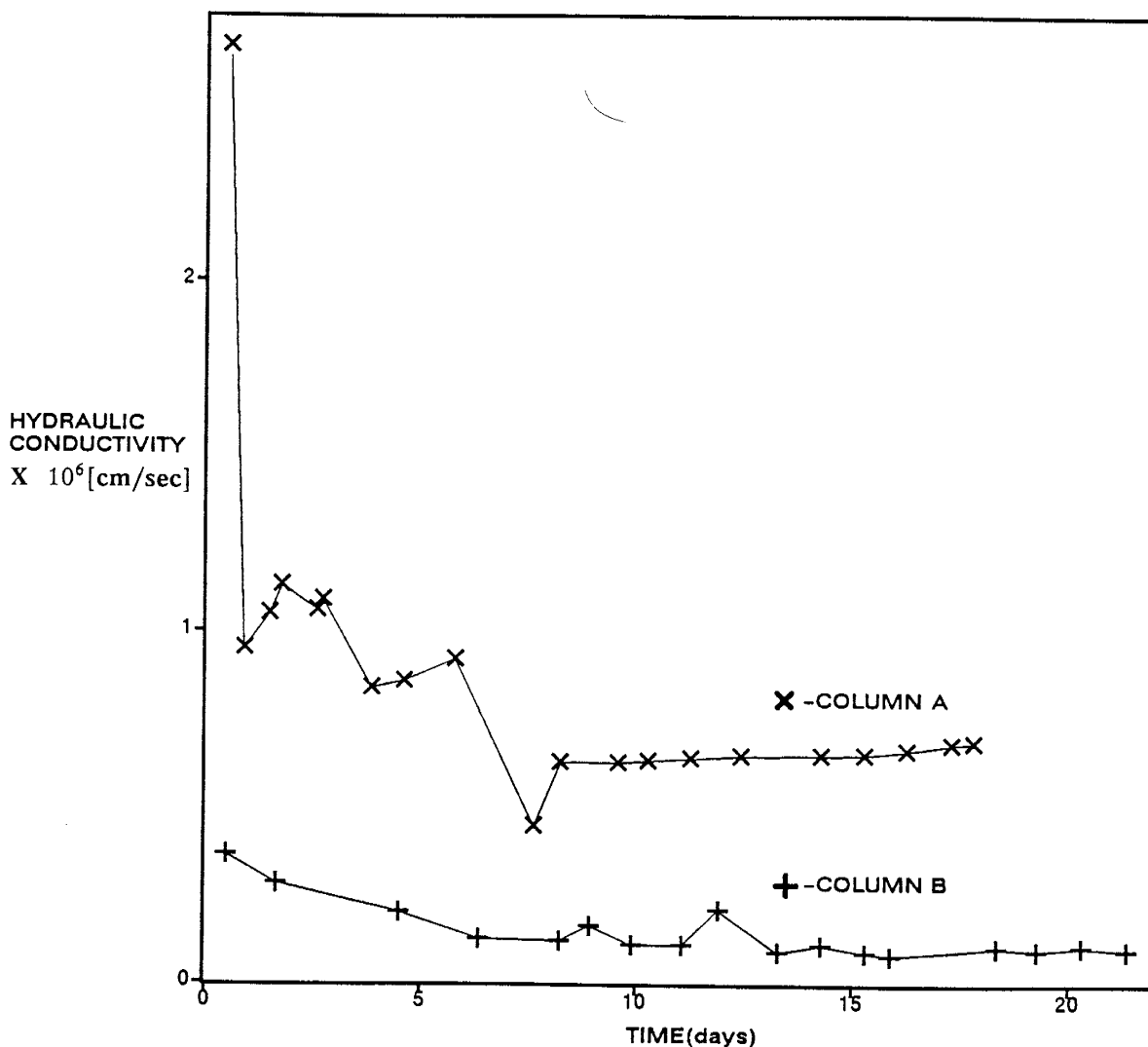
FIGURE 3-4. STABILIZATION GRAPHS FOR COLUMNS A AND B.

Only two of the three columns originally intended for these experiments were successful. The third column, column C, yielded hydraulic conductivity
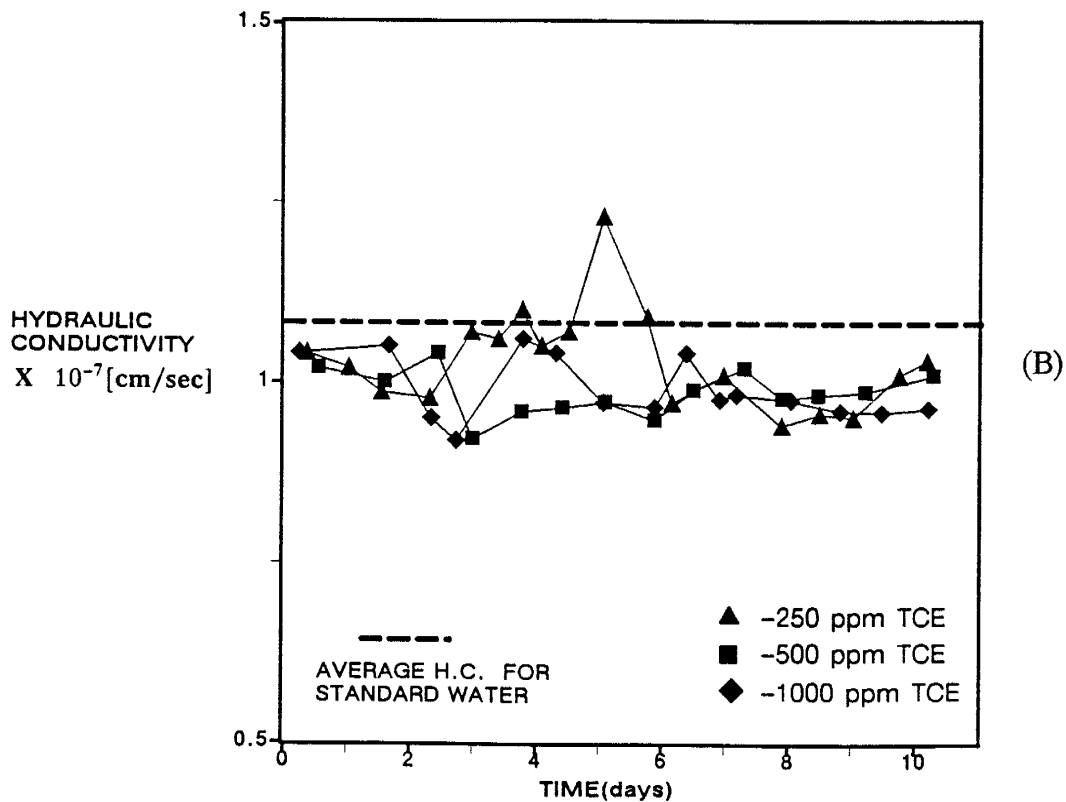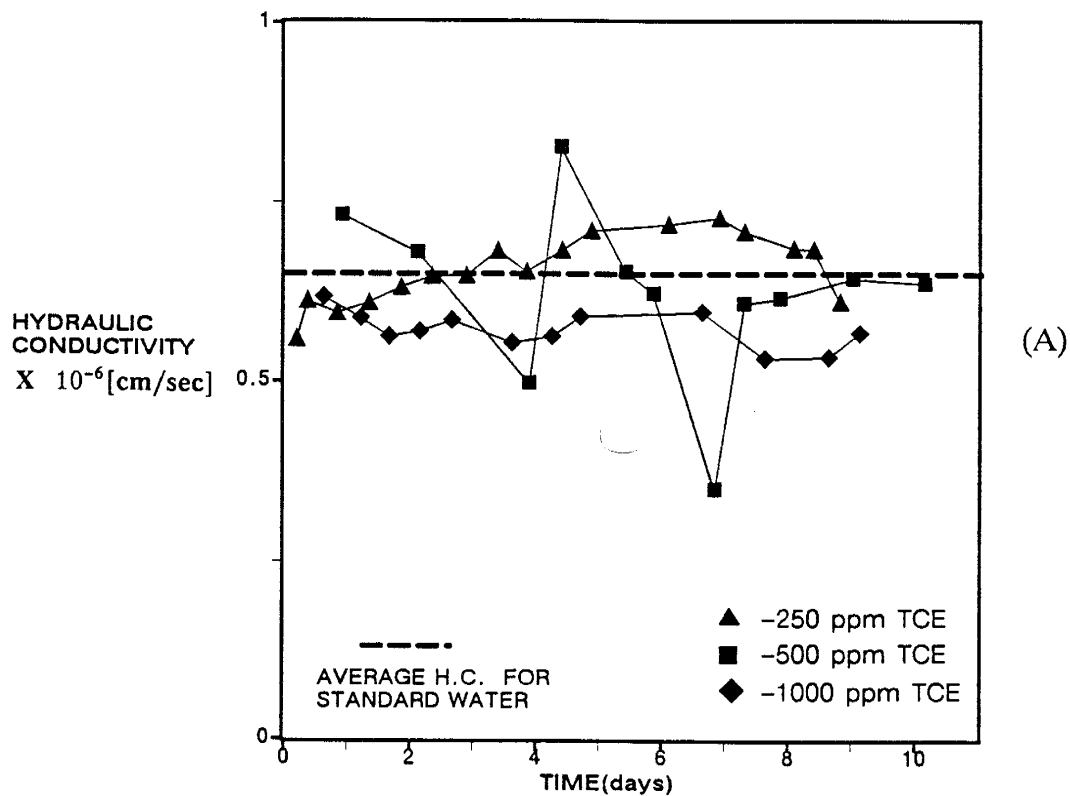
FIGURE 3-5. PLOT OF TIME VS HYDRAULIC CONDUCTIVITY FOR (A)COLUMN A, (B)COLUMN B; IN TCE SOLUTIONS

values too low for the completion of the experiments in the designated time frame.

4.2 DISCUSSION

4.2.1 INTRACRYSTALLINE PHENOMENA

Discussion of the results of the intracrystalline expansion study must be examined in terms of the variables of each clay-organic system: 1) charge density of the clay surface, 2) interlayer cation, 3) hydration state of the interlayer cation, and 4) the properties of the organic compound. The charge density and interlayer cation are constant in their respective clay-organic complex because the intercalation of substances in the interlamellar space does not alter either of these properties. Further, the initial hydration state of the clay minerals is also constant since no measures were taken to dehydrate the clays prior to organic immersion, and the sample slides were all stored under the same conditions prior to organic immersion. Therefore, discussion will focus on the effect of the organic properties on the final c-axis dimension of the clay-organic complex, with distinctions being made for the two samples.

EFFECT OF THE CLAY SURFACE

As previously shown low-charge density clays have a greater propensity for expansion than do high-charge density clays because the work of expansion is less for low-charge density clays than for high-charge density clays. Table 3-1 reveals that the smectite fraction of the SV-15 clay minerals (henceforth referred to as the "SV-15 smectite") expands more than the STx-1 smectite in compounds with high dielectric constants and dipole moments, and the STx-1 smectite expands to a greater degree in solvents with low dielectric constants and dipole moments. The charge density of the SV-15 smectite is not known;

however, based on the knowledge that low–charge density smectites are more readily expandable than high–charge density smectites and that the STx-1 smectite is more expandable in low dielectric constant–low dipole moment solvents than the SV-15 smectite, and that the SV-15 smectite expands more than the STx-1 smectite in high dielectric constant–high dipole moment solvents could mean that the SV-15 smectite has a greater charge density than the STx-1 smectite.

The SV-15 smectite most likely has a higher permanent and pH–dependent layer charge than the STx-1 smectite based on the difference in their occurrence. The SV-15 smectite is of detrital origin in which the weathering environment is conducive to the exchange of higher valence cations for lower cations, and hence, increase permanent charge deficiencies in the crystal structure. Further, abrasion of the clay minerals with other grains during transport and deposition serves to break bonds at the crystal edges and open pH–dependent charge sites. The broad diffraction maxima of the SV-15 smectite compared to the STx-1 smectite indicates that it is of lower relative crystallinity, and that pH–dependent layer charge may add significantly to the overall layer charge of the SV-15 smectite.

The STx-1 montmorillonite resulted from the *in situ* alteration of a volcanic ash of rhyolitic composition (van Olphen and Fripiat, 1979). The resulting bentonite is chemically homogeneous (van Olphen and Fripiat, 1979) indicating that the fluids responsible for the alteration from ash to bentonite were also chemically homogeneous which sets a limit on the degree isomorphous substitution in the smectite structure. This combined with the fact that the bentonite itself has not been transported, and therefore not mechanically abraded, has resulted in a highly crystalline smectitic material. Thus, pH–dependent charge

sites do not contribute significantly to the overall charge density of the STx-1 smectite.

In figures 3-6 to 3-8 in which data from the SV-15 and STx-1 clay-organic complexes are plotted separately, the absolute value of the slope of the best fit line is greater for the the SV-15 smectite in every case. This further confirms that the SV-15 smectite expands more in polar solvents and less in nonpolar solvents than the STx-1 smectite. The higher layer charge of the SV-15 smectite allows for more adsorption of polar compounds in the interlayer, and a c-axis dimension which is greater for SV-15 clay-polar organic complexes than STx-1 clay-polar organic complexes for the same polar solvent.

In conclusion, based on their swelling characteristics and their occurrences, of the two smectites the SV-15 probably carries the higher layer charge. However, because of their very different genetic histories from this study the SV-15 smectite can not irrevocably be said to have the higher charge density.

EFFECT OF THE INITIAL HYDRATION STATE ON EXPANSION

The smectites used in this study were not dehydrated prior to immersion in the organic fluids in contrast to the work of Barshad (1952), Norrish (1954), Olejnik et al. (1974), and Berkheiser and Mortland (1975). All of the solvents used in this study caused a change in the c-axis dimension relative to the air-dried c-axis dimension of both the SV-15 and the STx-1 smectites, indicating that clay-organic complexation had occurred in the interlayer. Barshad (1952) found that smectites dehydrated at 250°C did not form complexes with benzene or n-hexane. Both of these solvents are nonpolar and will not readily hydrate
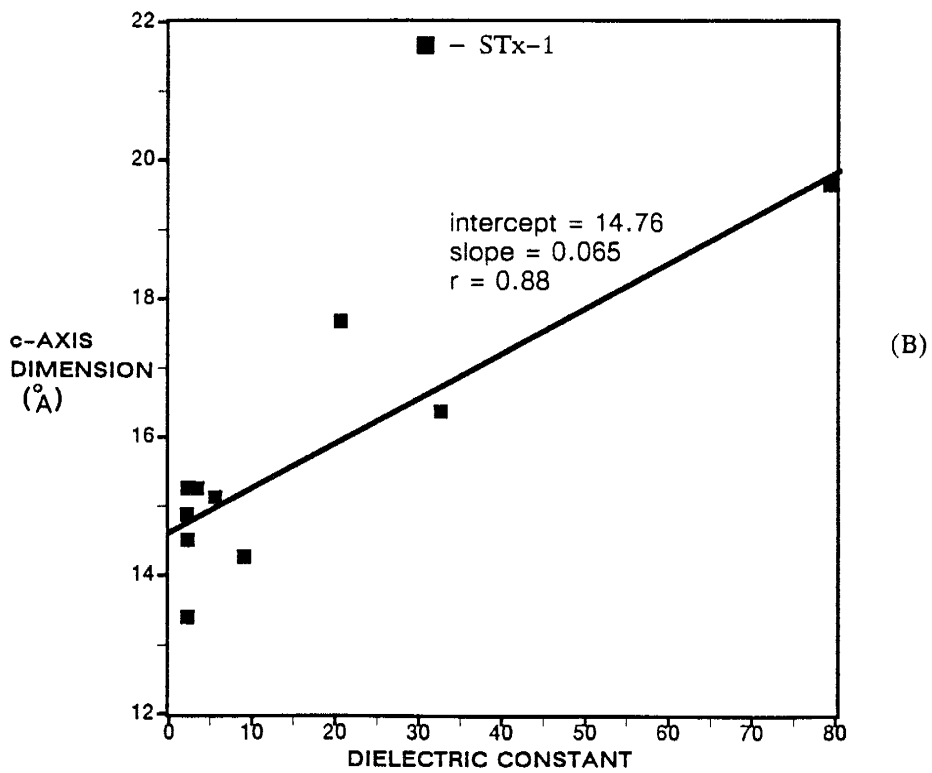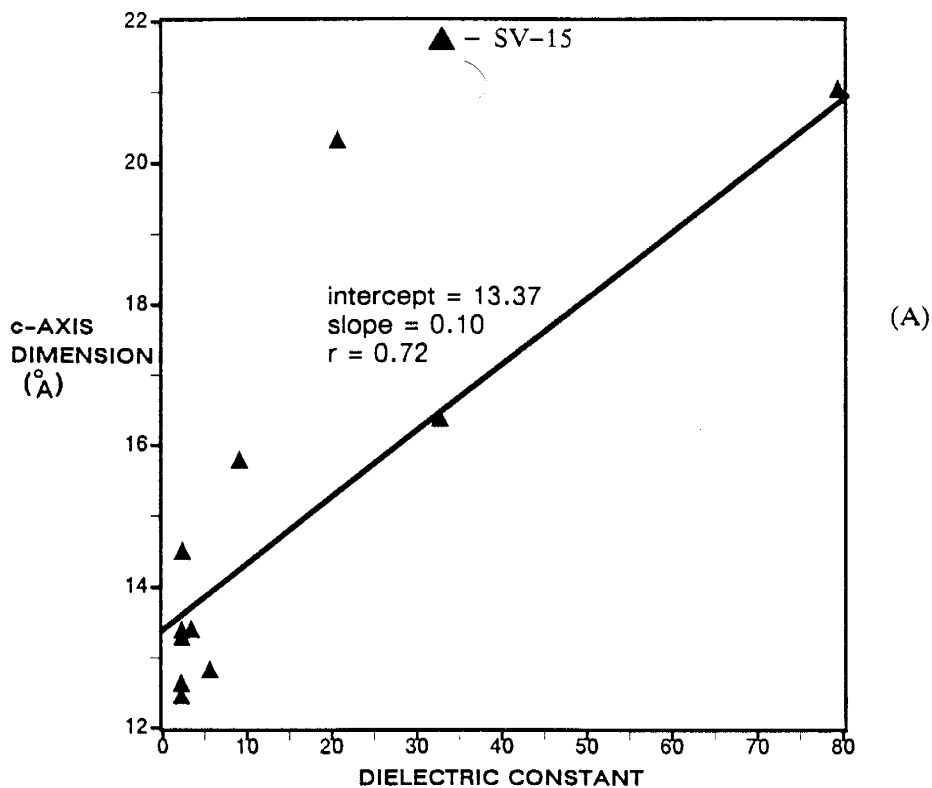
FIGURE 3-6. DIELECTRIC CONSTANT VS C-AXIS DIMENSION
(A) SV-15 SMECTITE, (B) STx-1 SMECTITE
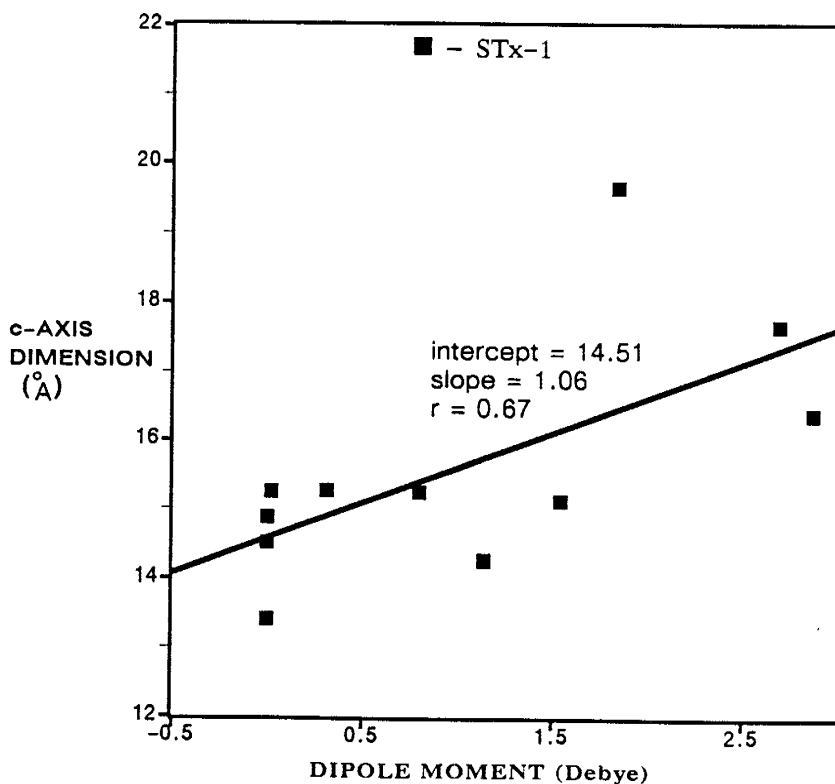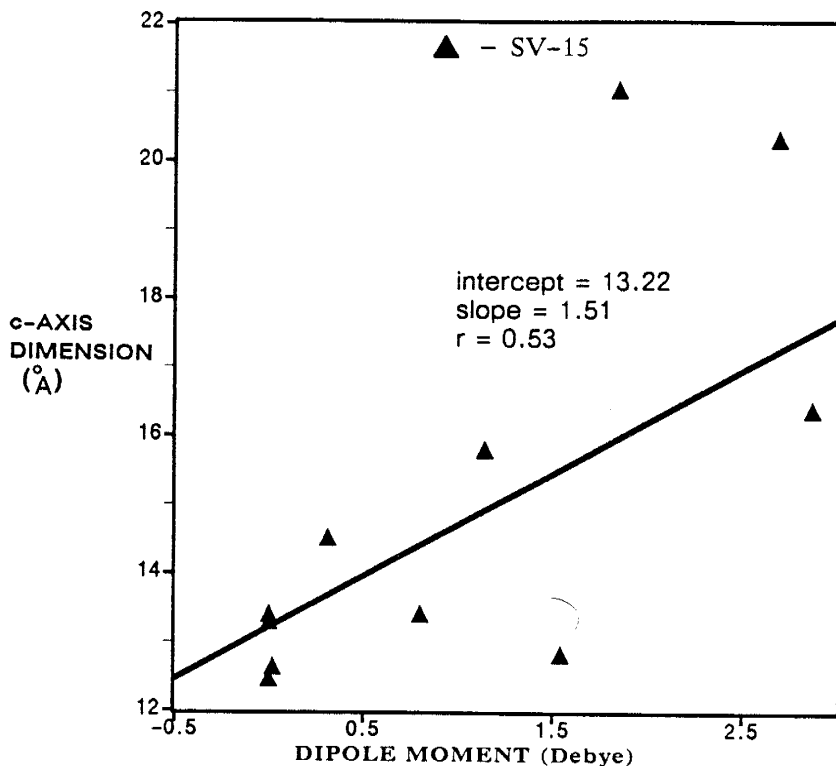
FIGURE 3-7. DIPOLE MOMENT VS C-AXIS DIMENSION
(A) SV-15 SMECTITE, (B) STx-1 SMECTITE.
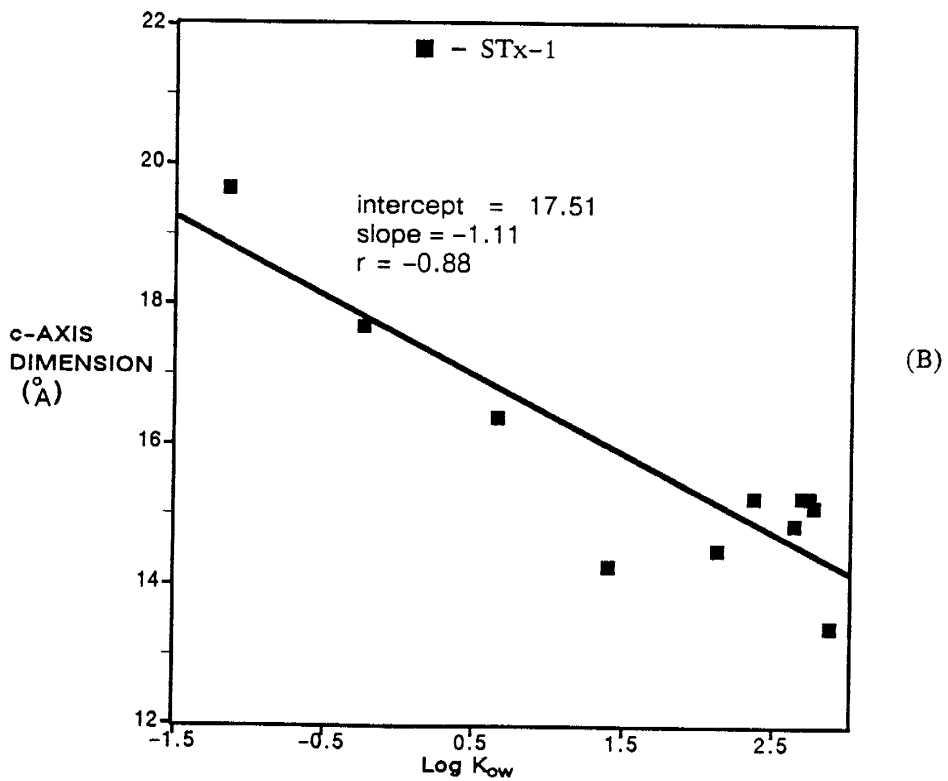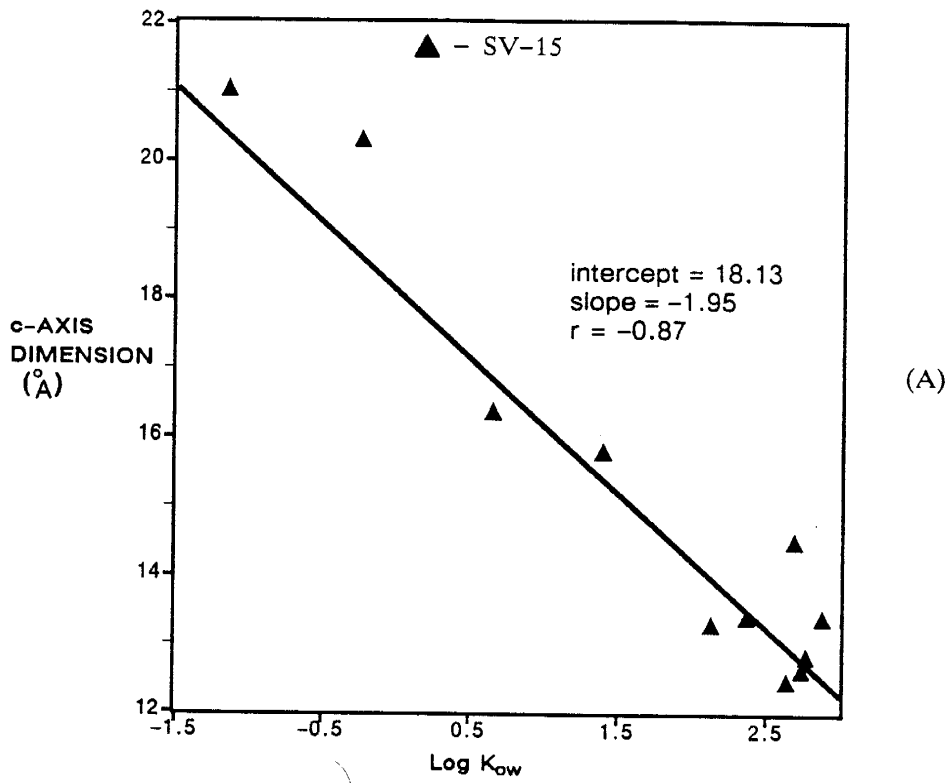
FIGURE 3-8. LOG K_{ow} VS C-AXIS DIMENSION (A)
SV-15 SMECTITE, (B) STx-1 SMECTITE.

an ionic or charged site (interlayer and interlayer cation). The most probable reason Barshad (1952) did not observe any complexation with nonpolar compounds and smectites with collapsed structures was because the hydration energy of the organic–clay–cation system was not great enough to overcome the energy necessary to expand the collapsed structure. However, Barshad (1952) found that polar compounds (e.g., acetone, ethanol, n–butanol, and diethyl ether) could expand smectites that had been dehydrated at 250°C.

Soil temperatures normally do not exceed 250°C in most near–surface geologic environments. The natural state of smectites in these environments will most likely be hydrated to a limit determined by the available moisture and the hydration characteristics of the clay. Because they are hydrated clays which encounter organic contamination in a natural environment may undergo an alteration of their physical properties from a change in the chemistry of the pore fluids.

CHEMICAL PROPERTY EFFECTS

The chemical properties of the interlayer medium, the dielectric constant, dipole moment, and log K_{ow} have a direct influence on the physical dimensions of smectite clays (Table 3–1).

(A) *300 ppm CaCl$_2$ aqueous solution, and TCE dilutions.* The 300 ppm CaCl$_2$ and TCE aqueous solutions caused the greatest amount of swelling of both the SV–15 and STx–1 smectites. Because water has the unique characteristics of a low molecular weight and combined with a high dielectric constant and a relatively high dipole moment makes the adsorption of multiple layers of water in the interlayer possible. The water–TCE dilutions did not cause any measurable alteration of the c–axis dimension of the clay complex as compared

to that measured for water with 300 ppm $CaCl_2$. The addition of small amounts of TCE was probably not significant in changing the properties of the bulk solution and the properties of the water dominated the behavior of the system.

(B) *Methanol.* Methanol, a polar alcohol completely miscible in water, caused collapse of the experimental clays with respect to water. The decreased dielectric constant and higher molecular weight of methanol with respect to water most probably caused the observed collapse.

The behavior of clay–methanol and clay–acetone complexes can not be predicted from consideration of their dielectric constants. Based on the dielectric theory one would predict that smectite–methanol complexes would yield final c–axis dimensions greater than those of smectite–acetone complexes. Both the SV–15 and the STx–1 acetone complexes had final c–axis dimensions which were greater than their respective complexes in methanol. This might be explained in terms of methanol having a higher dipole moment than acetone resulting in closer packing of the methanol molecules in the interlayer than is possible for acetone. The end result of the tighter packing is a smectite–methanol complex which has a final c–axis dimension less than smectite–acetone complexes.

(C) *Acetone.* Acetone, a polar organic solvent which is completely miscible in water, caused the SV–15 and the STx–1 smectites to collapse relative to water. Although acetone has a higher dipole moment than water, thus, increasing dipole–dipole interactions of acetone in the interlayer relative to water, it also has a lower dielectric constant and higher molecular weight which offset the increased dipole effects.

(D) *Dichloromethane.* Dichloromethane is a slightly polar organic solvent that is very soluble in water (13,200 mg/l at 20°C; Griffin and Roy, 1985). This solvent caused collapse of the smectite structure for the SV–15 and the STx–1 samples relative to water, methanol and acetone. The decreased dielectric constant and dipole moment of dichloromethane relative to the solvents discussed here are indicators as to the observed behavior of the smectite-dichloromethane complexes.

(E) *Chlorobenzene.* Chlorobenzene is a slightly polar aromatic hydrocarbon with a low aqueous solubility (448 mg/l at 30°C; Griffin and Roy, 1985). With the exception of STx–1–dichloromethane complex, the final c–axis dimension of the smectite–chlorobenzene complexes were less than those of the prior smectite–organic complexes. The discrepancy between the STx–1–chlorobenzene and the STx–1–dichloromethane complexes may be explained in terms of the higher dipole moment of chlorobenzene than for dichloromethane. Chlorobenzene with a higher dipole moment can form a tighter packing arrangement in the interlayer resulting in the final c–axis dimension, one less for STx–1–chlorobenzene complexes than for STx–1–dichloromethane complexes. This behavior, however, does not occur for the SV–15–dichloromethane-chlorobenzene complexes because of the higher charge density of the SV–15 smectite and the difference in the aqueous solubility of chlorobenzene and dichloromethane. The higher charge density increases the force of attraction between the silicate layers and the interlayer cation, and thus so increases the work of expansion. Therefore, in order to expand a high charge density structure the energy of hydration of the clay–organic–cation system must be greater than the work of expansion. Since dichloromethane has a much higher aqueous

solubility than chlorobenzene its energy of hydration is also greater and the end result is a clay–organic complex of greater dimension.

(F) *Benzene.* Benzene, a nonpolar aromatic hydrocarbon that is moderately soluble in water (approximately 1800 mg/l at 25°C), caused collapse of both the smectites relative to water, and relative to the other solvents with the exception of SV–15–benzene–chlorobenzene complexes. Benzene has a lower dielectric constant and dipole moment than chlorobenzene and should cause the c–axis dimension to decrease relative to chlorobenzene for the same clay, however, this is not the case; the combined affects of high charge density of the SV–15 smectite, higher aqueous solubility of benzene, and the dipolar packing chlorobenzene resulted in SV–15–benzene complexes to achieve greater c–axis dimensions than SV–15–chlorobenzene complexes.

(G) *Toluene.* Toluene is a slightly polar aromatic hydrocarbon which is slightly soluble in water (approximately 500 mg/l at 20°C; Griffin and Roy, 1985). For both smectite–toluene complexes the final c–axis dimension was less than their respective complexes with water. Smectite–toluene complexes yielded final c–axis dimensions which were consistent with the theories of the dielectric and the dipole moment.

(H) *P–xylene.* P–xylene is a nonpolar aromatic hydrocarbon that has a very low aqueous solubility (approximately 180 mg/l at 20°C; Griffin and Roy, 1985). The complexes formed with the clays and p–xylene yielded final c–axis dimensions less than those formed with water–saturated clays. The decreased c–axis dimension of p–xylene complexes with respect to toluene complexes are a function of toluene having a larger dielectric constant.

(I) *Carbon Tetrachloride.* Carbon tetrachloride is an aliphatic chlorinated hydrocarbon with a moderately low aqueous solubility (800 mg/l at 25°C; Griffin and Roy, 1985). Complexes formed with CCl_4 and the experimental clays gave c-axis dimensions less than those in water. The CCl_4 complex formed with the SV-15 smectite yielded the a c-axis dimension which was the least of all the clay-organic complexes in this study. The absence of a dipole on the CCl_4 molecule and the presence of four chlorine atoms, which hydrogen bond to the interlayer water may explain why this clay-organic complex had the most collapsed structure. The STx-1-CCl_4 complex yielded a c-axis dimension which was not as collapsed as that for the SV-15 complex which is consistent with the decreased charge density of the STx-1 smectite.

(J) *Trichloroethene.* Trichloroethene, an unsaturated aliphatic chlorinated hydrocarbon that has a moderate aqueous solubility (1000 mg/l at 25°C; Griffin and Roy, 1985), caused the structures of both the SV-15 and STx-1 smectites to collapse relative to water. The swelling behavior of clay-TCE complexes is adequately explained in terms of the dielectric and dipole moment theories.

(K) *Tetrachloroethene.* Tetrachloroethene is an unsaturated aliphatic chlorinated hydrocarbon which has a low aqueous solubility (150 mg/l at 25°C; Griffin and Roy, 1985). Relative to water, tetrachloroethene caused the c-axis dimension of the smectites to decrease. This decrease is predicted from PCE's low dielectric constant and nonexistent dipole moment. The STx-1-PCE complex yielded the smallest c-axis dimension for that clay. Contributions from the surface properties of the clay, the high molecular weight of PCE, and the low solvation of PCE act to diminish its ability to expand the STx-1.

SIGNIFICANCE OF THE LOG K_{ow} RELATIONSHIP

The log K_{ow} is plotted against the aqueous solubility for the organics used in this study in Figure 3-9a. The negative straight line correlation indicates that as the log K_{ow} increases the solubility of the organic compound in water decreases. This implies that the log K_{ow} of a compound is a direct reflection of its aqueous solubility; however, the aqueous solubility of the organic compounds is plotted against the c-axis dimension of the clay-organic complexes in Figure 3-9b. It is obvious from Figure 3-9b that there is little if any correlation between the the c-axis dimension of the clay-organic complexes and the aqueous solubility of the organic compounds. Therefore, the log K_{ow} must also represent another property of water-organic interactions which is not as obvious as the aqueous solubility.

Since the propensity for a clay to expand or contract when in contact with a liquid is a function of two opposing forces, the force of repulsion (i.e., the total hydration energy of the liquid-clay surface-cation system) and the force of attraction of the negatively charged silicate layers for the interlayer cation (i.e., the work of expansion), the log K_{ow} must represent an energy term. Perhaps the log K_{ow} of a compound represents an energy coefficient of that compound's affinity for nonpolar to polar environments. This seems like a valid conclusion in consideration of the definition of K_{ow} which is the ratio of the concentrations of a compound in n-octanol (nonpolar environment) to water (polar environment).

In terms of clay-organic complexation, where the organic is present in the free organic phase, the clay interlayer would classify as the polar environment and the free organic phase as the nonpolar environment. This was the situation in the experimental procedure employed in the crystalline expansion
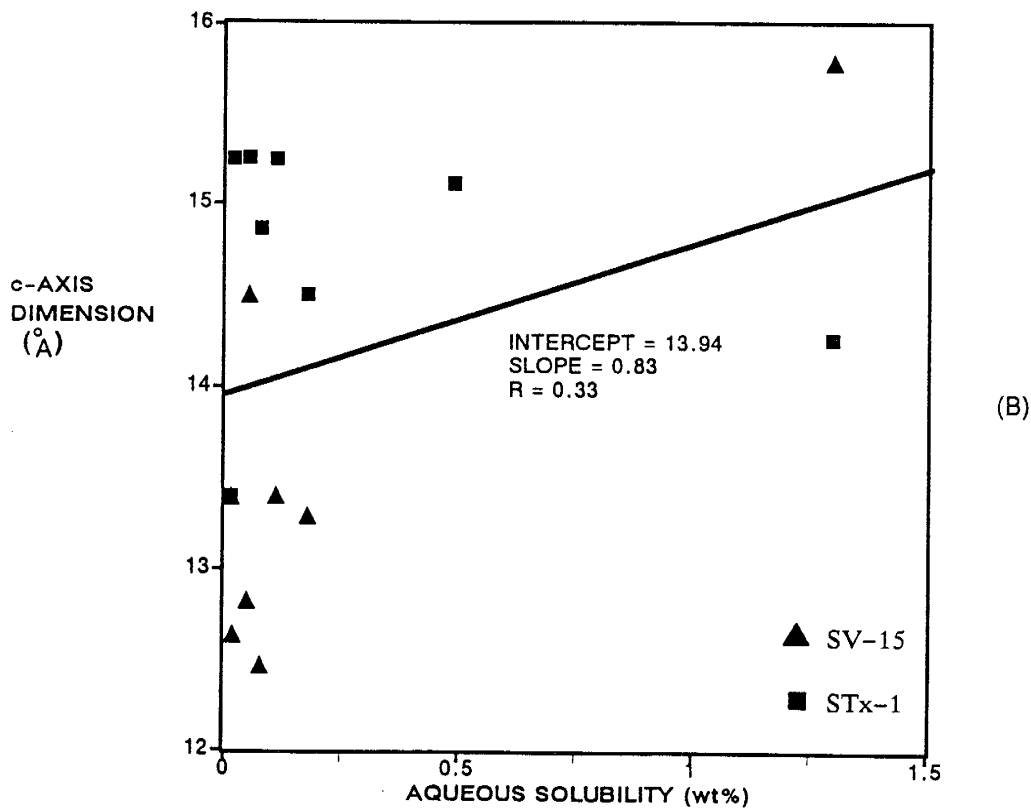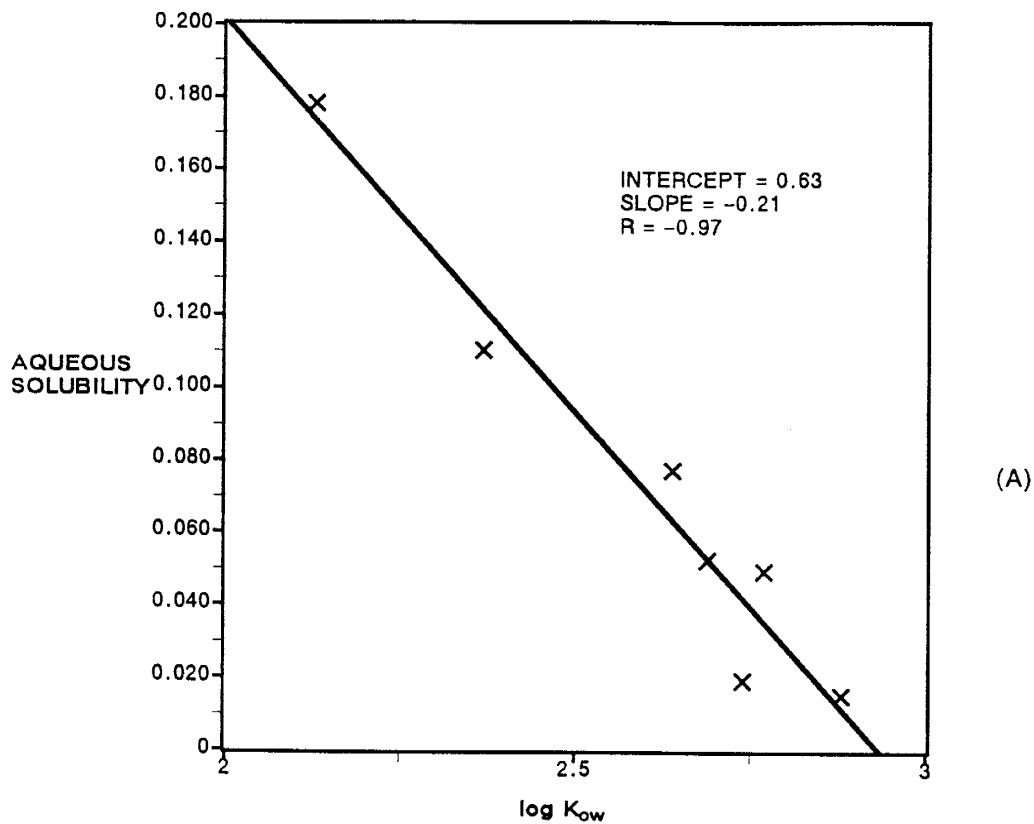
FIGURE 3-9 . (A) PLOT OF LOG K_{ow} VS AQUEOUS SOLUBILITY, (B) PLOT OF AQUEOUS SOLUBILITY VS C-AXIS DIMENSION.

phase of this study, however, in systems where the organic is present as a dissolved aqueous species, definition of the polar environment may be dependent upon the charge density of the clay surface and the ionic strength of the solution. Regardless of the exact meaning of the log K_{ow} in terms of organic–inorganic interactions, it remains as the one parameter of organic compounds which best predicts the affect on the swelling characteristics of smectite–organic complexes.

ORGANIC COMPLEXES WITH NON–EXPANDING LATTICE CLAYS

With the exception of acetone, all of the compounds in Table 3–2 that formed complexes with non–expanding lattice minerals are chlorinated. This indicates that the formation of hydrogen bonds between the chlorine of the organic and the hydrogen of the adsorbed water may be the mechanism responsible for the formation of these complexes. The values of the crystallinity index are semiquantitative at best, and should only be used as indication of which compounds formed complexes with the non–expanding clay minerals.

4.2.2 COLUMN PHENOMENA

The results presented at the beginning at of this chapter are in general agreement with the hydraulic conductivity values that Black and Veatch Consulting Engineers (1988) and Hart Associates Inc.(1988) calculated for the shallow aquitard at the SJ–6 site. Black and Veatch Consulting Engineers (1988) and Hart Associates Inc.(1988) reported hydraulic conductivities of 1–6 x 10^{-7} cm/s which are within the range of values that the column study gave for the hydraulic conductivity.

Neither of the columns showed any systematic or significant changes in the hydraulic conductivity when saturated with TCE solutions, the reason being

that at concentrations up to the aqueous solubility limit of TCE (approximately 1000 mg/l) the effect of TCE on the properties of the bulk solution are probably negligible, and therefore the effect on the physical properties of the clay are also negligible.

Column A has a mean hydraulic conductivity which is greater by a factor 6 than column B. The discrepancy between the hydraulic conductivities of the two columns can be explained in terms of the differences in the physical properties of the columns. The porosity of column A, 0.48, is greater than the 0.46 value of column B, and the porosity can have a controlling influence on the hydraulic conductivity (Freeze and Cherry, 1979).

The hydraulic conductivity of column C yielded values in the range of 10^{-10} cm/s. Column C had physical properties which were intermediate between columns A and B; therefore, air entrapped in the pore spaces of the porous media is probably responsible for the lower hydraulic conductivity of column C. Even after stabilization times of greater than one month the hydraulic conductivity did not increase to values comparable to the other columns. No attempts were made to correct the situation and the column was abandoned for the remainder of the experiments.

In the final phase of the column study, the columns were to be saturated with pure organic phase TCE to monitor its affect on the hydraulic conductivity of the clay system. Since TCE is only slightly soluble in water it exists as the non-wetting immiscible phase in the water-clay-organic system, the minimum capillary pressure of displacement for TCE and water is given by:

$$P_c = \frac{4\sigma\cos\theta}{D}$$

where,

$$\sigma = 34.5 \text{ dynes/cm (TCE–water)} \qquad \text{(Demond, 1988)}$$

$$\theta = 38 \pm 3° \text{ (TCE–water)} \qquad \text{(Demond, 1988)}$$

$$D = 6 \times 10^{-6} \text{cm (compacted kaolinite)} \qquad \text{(Acar, 1985)}$$

$$P_c = 1.81 \times 10^7 \quad \text{dynes/ cm2}$$

$$= 18 \text{ atm}$$

Converting to an equivalent head using the equation for hydrostatic pressure;

$$P = \varrho \; g \; h$$

where,

ϱ = density of the fluid.

g = acceleration due to gravity.

h = height of the fluid column.

and solving for h yields an equivalent elevation of TCE equal to approximately 13 meters. Calculation of the capillary displacement pressure is only a rough approximation of pressures to be expected in actual laboratory or field situations. Sources of error in this calculation are in the measurement of the parameters of; contact angle, interfacial tension, and the pore diameter (S. Conrad, personal communication, 1989). To determine the actual capillary pressure of displacement for a particular immiscible phase in a given geologic material,

saturation–capillary pressure experiments must be performed, for further discussion on this and immiscible flow see Hagan (1989) and Demond (1988).

The pressure required to displace water with TCE is extreme in clay–dominated systems, and that in the laboratory special experimental apparatus is necessary to perform such high pressure experiments. These pressures would probably never be achieved in near surface geologic environments of contaminated sites, and clay barriers can be effective in preventing the migration of immiscible compounds.

CHAPTER 4

SUMMARY AND CONCLUSIONS

CONCLUSIONS OF THE INTRACRYSTALLINE SWELLING STUDY

• All of the organic compounds used in this study caused a shrinkage in the c-axis direction of the experimental smectites relative to water.

• Based on this study the SV-15 smectite probably carries a greater layer charge density than the STx-1 smectite.

• The initial hydration state of the smectite prior to organic immersion determines whether or not formation of organic complexes with nonpolar solvents will occur.

• The aqueous solutions caused the greatest amount of swelling of both the SV-15 and STx-1 smectites. However, the two smectites did not react identically to all of the solvents as the series of increasing c-axis dimension indicates. For the SV-15: carbon tetrachloride < p-xylene < chlorobenzene < benzene < tetrachloroethene < trichloroethene < toluene < dichloromethane < acetone < methanol. For the STx-1: tetrachloroethene < dichloromethane < benzene < chlorobenzene < carbon tetrachloride < trichloroethene = p-xylene < toluene < methanol < acetone.

• The dielectric constant of the organic liquids showed a moderate positive correlation (r = 0.74) to the c-axis dimension of the clay-organic complexes. The swelling behavior of the STx-1 smectite

could be better predicted from the solvents dielectric constant than the SV–15 smectite.

- The dipole moment, as a single criterion, is not a good indication of how a solvent will affect the c–dimension of smectites.

- The log K_{ow} of a solvent is the most reliable solvent property to predict the c–dimension of smectite–organic complexes.

- Formation of clay–organic complexes with non–expanding lattice clays occurs, and most frequently with chlorinated hydrocarbons.

CONCLUSIONS OF THE COLUMN STUDY

- The measured hydraulic conductivity of the SV–15 clay material agrees with values from the consultant reports.

- The aqueous solutions of TCE had no measurable effect on the hydraulic conductivity of the SV–15 clay material.

- TCE did not cause macropores to form in the SV–15 clay material in the laboratory.

- Immiscible organics will alter the hydraulic properties of a clay dominant system only if the capillary pressure of displacement is achieved.

- Mixtures of miscible and immiscible (with water) solvents are more likely to cause alterations of the hydraulic properties of clays than purely immiscible solvents.

RECOMMENDATIONS FOR FUTURE STUDIES

The original goal of this study was to relate the microscale swelling phenomena of smectite in TCE to the observed changes in the hydraulic conductivity of the clay system, and then to extrapolate the effects of other organic compounds on the hydraulic conductivity based on the organic's chemical properties and the effect they had on the c-axis dimensions of the clay-organic complexes. This goal was proved elusive due to the unforseen effects of TCE's immicibility with water, but future research using a miscible organic such as acetone or methanol in place of TCE for the column studies could possibily achieve this goal.

REFERENCES

Acar, Y. B., Olivieri, I., and Field, S. D., (1985) The effects of organic fluids on the pore size distribution of compacted kaolinite, in Hydraulic Barriers in Soil and Rock: A. I. Johnson, R. K. Frobel, N. J. Cavalli, and C. B. Pettersson, eds., American Society for Testing and Materials, Philadelphia, ASTM STP 874, 203-212.

Alperovitch, N., Shainberg, I., and Keren, R., (1981) Specific effect of magnesium on the hydraulic conductivity of sodic soils: *J. Soil Sci.* **32**, 543-554.

Anderson, D., and Brown, K. W., (1981) Organic leachate effects on the permeability of clay liners: in *Land Disposal of Hazardous Waste,* Proceedings of the Seventh Annual Research Symposium, U.S. Environmental Protection Agency EPA-600/9-81-002b. 119-130.

Barshad, I., (1950) The effect of the interlayer cations on the expansion of the mica type crystal lattice: *Amer. Min.* **35**, 225-238.

Barshad, I., (1952) Factors affecting the interlayer expansion of vermiculite and montmorillonite with organic substances: *Soil Sci. Soc. Amer. Proc.* **16**, 176-182.

Bear, J., (1972) *Dynamics Of Fluids In Porous Media,* Dover ed.,: Dover Publications Inc., New York, 764 pp.

Berkheiser, V., and Mortland, M. M., (1975) Variability in exchange ion position in smectite: dependence on interlayer solvent: *Clays and Clay Minerals* **23**, 404-410.

Black and Veatch, Consulting Engineers, (1988) Draft, remedial investigation report, SJ-6 Superfund site, South Valley area, Albuquerque, NM, 9.6L11.0/W633181: consultant report prepared for the USEPA, Hazardous site control division, variously paginated.

Brindley, G. W., (1980) Intracrystalline swelling of montmorillonites in water-dimethylsulfoxide systems: *Clays and Clay Minerals* **28**, 369-372.

G. W. Brindley and G. Brown Eds., (1980) *Crystal Structures of Clay Minerals and their X-ray Identification,* Mineralogical Society Monograph No. 5, 495 pp.

Brindley, G. W., Wiewora, K., Wiewora, A., (1969) Intracrystalline swelling of montmorillonite in some water-organic mixtures: (Clay organic studies XVII), *Amer. Min.* **54**, 1635-1644.

Bryan, K., (1938) Geology and ground-water conditions of the Rio Grande depression in Colorado and New Mexico: Washington Regional Planning, pt. 6, Rio

Grande joint inv. upper Rio Grande Basin, National Resource Committee, **1**, pt. 2, sec. 1, 197–225.

Chapin, C. E., and Seager, W. R., (1975) Evolution of the Rio Grande Rift in the Socorro and Las Cruces areas: New Mexico Geol. Soc., Guidebook **26**[th] field conf., 297–321.

Chiou, C. T., Peters, L. J., and Freed, D. W., (1979) A physical concept of soil-water equilibria for nonionic organic compounds: *Science* **206**, 831–832.

Davidtz, J. C., and Low, P. F., (1970) Relation between crystal–lattice configuration and swelling of montmorillonites: *Clays and Clay Minerals* **18**. 325–332.

Demond, A. (1988) Capillarity in two–phase liquid flow of organic contaminants in groundwater: unpublished ph.D dissertation, Stanford University, 65–85.

Drever, J. I., (1973) The preparation of oriented clay mineral specimens for X–ray diffraction analysis by a filter–membrane peel technique: *Amer. Min.* **58**, 553–554.

Freeze, R. A., and Cherry, J. A., (1979) *Groundwater:* Prentice Hall Inc., New Jersey, 604 pp.

Giese, R. F., (1988) Kaolin Minerals: Structures and Stabilities, in *Hydrous Phyllosilicates:* S. W. Bailey, ed., Reviews in Mineralogy **19**, Mineralogic Society of America, 29–66.

Guven, N. (1988) Smectites, in *Hydrous Phyllosilicates:* S. W. Bailey, ed., Reviews in Mineralogy **19**, Mineralogic Society of America, 497–560.

Green, W. J., Lee, G. F., and Jones, R. A., (1981) Clay–soils permeability and hazardous waste storage: *Journal of Water Pollution Control Federation* **53**, 1347–1354.

Green, W. J., Lee, G. F., Jones, R. A., and Palit, T., (1983) Interaction of clay soils with water and organic solvents: Implications for the disposal of hazardous waste: *Environ. Sci. Technol.* **17**. 278–282.

Griffin, R. A., and Roy, W.R., (1985) Interaction of organic solvents with saturated soil–water systems: Environmental Institute for Waste Management Studies, University of Alabama, Open file report no. 3, 86 pp.

Hagan, E. F., (1989) A quantitative experimental investigation of the physical processes responsible for determining residual organic liquid saturations in porous media: Geoscience/Hydrology Section Open File Report **89–4**, New Mexico Institute of Mining and Technology, 160 pp.

Hart Associates Inc., Consulting Engineers, (1988) remedial investigation report, SJ-6 Superfund site, South Valley area, Albuquerque, NM, 3rd draft, consultant report prepared for the USEPA, Hazardous site control division, variously paginated.

Huheey, J. E., (1978) *Inorganic Chemistry: Principles of Structure and Reactivity*, Harper and Row, New York, 889 pp.

Karicknoff, S. W., Brown, D. S., and Scott, T. A., (1979) Sorption of hydrophobic pollutants on natural sediments: *Water Resource* **13**, 241–248.

Kelley, V. C., (1977) Geology of the Albuquerque Basin, New Mexico: New Mexico Bureau of Mines and Mineral Resources, Memoir 33, 60 pp.

Kenaga, E. E., and Goring, C. A. I., (1980) Relationship between water solubility, soil sorption, octanol–water partitioning, and concentration of chemicals in biota, in *Aquatic Toxicology*: J. G. Eaton, P. R. Parrish, and A. C. Hendricks Eds., American Society of Testing and Materials, ASTM STP 707, 78–115.

Klute, (1986) *Methods Of Soil Analysis*, Part I. 2nd ed., Soil Science of America Inc., Madison, Wis. 1188 pp.

Lagaly, G., and Weiss, A., (1969) Determination of the layer charge in mica–type layer silicates: *Proc. Int. Clay Conf.*, Tokyo **1**, 61–80.

McQuillan, D.M., (1982) Pollution of the Rio Grande valley fill aquifer: New Mexico Geol. Soc. Guidebook. 33rd field conf., Albuquerque County II. p.357–360.

Mingelgrin, U., and Gerstl, Z., (1983) Reevaluation of partitioning as a mechanism of nonionic adsorption in soils: *J. Environ. Qual.* **12**, 1–11.

Murray, R. S., and Quirk, J. P., (1982) The physical swelling of clays in solvents: *Soil Sci. Soc. Amer. J.* **46**, 865–868.

Norrish, K., (1954) The swelling of montmorillonite: *Disc. Farad. Soc.* **18**, 120–134.

Olejik, S., Posner, A. M., and Quirk, J. P., (1974) Swelling of montmorillonite in polar organic liquids: *Clays and Clay Minerals* **22**, 361–365.

Olson, R. E., and Daniel, D. E., (1981) Measurement Of The Hydraulic Conductivity Of Fine–grained Soils, in *Permeability and Groundwater Contaminant Transport*: T. F. Zimmie and C. O. Riggs, Eds., American Society for Testing and Materials, ASTM STP 746, 18–64.

Parker, F., Benefield, L. D., and Nelson, M. M., (1984) Effects of organic fluids on clay permeability: Purdue University, 41st Industrial Waste Conf. Proc., 283–292.

Office of Technology Assessment, (1984) *Protecting the Nation's Groundwater From Contamination,* Washington, DC: U.S. Congress, **OTA-O-233**.

Prost, R., (1975) : *Proc. Int. Clay. Conf.,* Mexico City, Mexico **1**, 351–365.

Pusch, R., and Carlsson, T., (1985) The physical state of pore water of Na–smectite used as a barrier component: *Eng. Geol.* **21**, 257–265.

Ravina, I., and Low, P. F., (1972) Relation between swelling, water properties and B–dimension in montmorillonite–water systems: *Clays and Clay Minerals,* **20**, 109–123.

Riddick, J. A., and Bunger, W. B., (1970) *Organic Solvents: Physical Properties and Methods of Purification 3rd ed.,* Techniques of Chemistry vol. II, Wiley–Interscience, New York, 1041 pp.

Ruehlicke, G., and Kohler, E. E., (1981) A simplified procedure for determining layer charge by the n–alkylammonium method: *Clay Minerals* **16**, 305–307.

Ruehlicke, G., and Niederbudde, E. A., (1985) Determination of layer–charge density of expandable 2:1 minerals in soils and loess sediments using the alkylammonium method: *Clay Minerals* **20**, 291–300.

Schramm, M., Warrick, A.W., Fuller, W.H., (1986) Permeability of soils to four organic liquids and water: Hazardous Wastes and Materials **3**, Mary Ann Liebert Pub., 21–27.

Senkayi, A. L., Dixon, J. B., Hossner, L. R., and Kippenberger, L. A., (1985) Layer charge evaluation of expandable soil clays by the alkylammonium method: *Soil Sci. Soc. Amer. J.* **49**, 1054–1060.

Shainberg, I., Alperovitch, N., and Keren, R., (1988) Effect of magnesium on the hydraulic conductivity of Na–smectite–sand mixtures: *Clays and Clay Minerals* **36**, 432–438.

Sposito, G., and Prost, R., (1982) Structure of water adsorbed on smectites: *Chem. Rev.* **82**, no. 6. 554–573.

Srodon, J., and Eberl, D. D., (1984) Illite, in *Micas*: S. W. Bailey, ed., Reviews in Mineralogy **13**, Mineralogic Society of America, 495–544.

Titus, F. B., (1982) Ground–water geology of the Rio Grande Trough in north–central New Mexico, with sections on the Jemez Caldera and the Lucero Uplift: New Mexico Geol. Soc., Guidebook 12th field conf., 186–192.

van Olphen, H., (1977) *An Introduction To Clay And Colloid Chemistry,* 2nd ed.,: Wiley, New York, 150–160.

van Olphen, H., and Fripiat, J. J., (1979) *Data Handbook For Clay Minerals And Other Non–metallic Minerals:* Peragammon Press, New York, 346 pp.

APPENDIX A

A-1 SAMPLE PROPERTY PROCEDURES

A-1.1 PARTICLE SIZE ANALYSIS

A-1.2 MOISTURE CONTENT

A-1.3 PARTICLE DENSITY

A-1.4 BULK MINERALOGY

A-1.5 CLAY MINERALOGY

A-2 SOLUTION PREPARATION

A-2.1 STANDARD WATER

A-2.2 TCE SOLUTIONS

A-3 COLUMN PROPERTIES

A-3.1 PORE VOLUME

A-1 SAMPLE PROPERTY PROCEDURES

A-1.1 PARTICLE SIZE ANALYSIS

The pipette method was employed to determine the percent sand, silt, and clay in the SV–15 sample. The procedure used is described in Klute (1986), and has been simplified by the elimination of pretreatments to remove calcium carbonate and organic matter. Preliminary tests proved carbonate and organic matter to be negligible in the SV–15 sample. The results of the particle size analysis are presented in section 3.1.2.

A-1.2 MOISTURE CONTENT

The moisture content of the SV–15 geologic material was determined several times in the course of this study. The method consisted of weighing the sample before and after drying in a 105°C oven for 24 hours, and calculating the moisture content from the relation given below.

$$\% \ water = [1 - \frac{sample \ weight_{dry}}{sample \ weight_{wet}}]x100$$

A-1.3 PARTICLE DENSITY

The particle density of the SV–15 material was determined in order to facilitate the calculation of the pore volume of the bulk sample in the column (Table A–1.3). The pycnometer method used is described in Klute (1986).

TABLE A-1.3

PARTICLE DENSITY

sample	trial #	temp °C	density water 1	moisture content	particle density 2	mean particle density 2
SV-15 6.0-8.5	1	24.5	0.99707	4.6 %	2.4458	2.51 ±0.06
	2	24.5	0.99707	4.6 %	2.5706	
	3	24.5	0.99707	4.6 %	2.5104	

[1] density of water (g/cm³) @ 25°C from: 1987 CRC Handbook of Physics and Chemistry

[2] particle density reported as g/cm³

A-1.4 BULK MINERALOGY

The bulk mineralogy of the SV-15 geologic material was determined using standard X-ray diffraction techniques which are described below.

The dried bulk SV-15 sample was carefully disaggregated in a mortar and pestle and sieved through a 200 mesh screen to a maximum particle size of 75μm. The sieved sample was then packed in a powder mount for X-ray examination. The sample was scanned from 2° to 60° 2θ at a scan speed of 2 degrees 2θ at 800 counts full scale, and 40 Kv and 25 mA. Primary mineralogic phases present were determined by comparing the positions of the diffraction maxima with standard tables. The results of the bulk mineralogy are given in section 3.1.2.

A-1.5 CLAY MINERALOGY

The mineralogy of the <2mm fraction of the SV-15 and STx-1 materials was determined using the X-ray diffraction techniques used at the New Mexico Bureau of Mines and Mineral Resources.

Oriented sample slides of the <2mm fraction were prepared using the filter peel technique of Drever (1973). In short, the <2µm fraction is collected as previously discussed, and filtered through a vacuum filter funnel equipped with a 45µm filter. After the water had passed, a thin oriented clay film remains on the filter which is placed, clay film down, on a glass petrographic slide. Using a centrifuge tube as a roller and rolling over the clay-filter composite the oriented clay film is transferred on to the slide. Upon drying at room conditions the sample slide is ready for X-ray examination.

The clay mineralogy of the samples was determined using the semi-quantitative approach used at the New Mexico Bureau of Mines and Mineral Resources. Three separate XRD records are required for this approach: an untreated record from 2° to 35° 2θ, an ethylene glycol-saturated record from 2° to 15° 2θ, and a heated record at 375°C covering, first, 8° to 9.8° 2θ, and 2° to 15° 2θ. The purpose of the ethylene glycol and heated runs is to isolate the diffraction maxima of smectite, illite and mixed-layer I/S. The following equations are used to quantify the data.

$$illite = \frac{I(1G)}{T} x 10$$

$$kaolinite = \frac{K(1)}{T} x 10$$

$$smectite = \frac{M(1)}{4T}x10$$

$$mixedlayer(I/S) = \frac{I(1H) - [I(1G) + \frac{M(1)}{4}]}{T}x10$$

where, T is the total counts

$$T = I(1H) + K(1)$$

and

K(1) is the diffraction maxima in counts of the 001 kaolinite peak above background.

M(1) is the diffraction maxima in counts of the glycolated 001 smectite peak above background.

I(1G) is the diffraction maxima in counts of the glycolated 001 illite peak above background.

I(1H) is the diffraction maxima in counts of the heated 001 illite peak above background.

The values obtained from this approach are reported as parts in ten i.e. percentage values with a standard deviation of $\pm 10\%$. Despite problems associated with quantitative clay analysis, the semi–quantitative approach yields easily reproducible results.

A-2 SOLUTION PREPARATION

A-2.1 PREPARATION OF STANDARD WATER

The 300 ppm $CaCl_2$ water used in every aspect of this study was prepared in the following manner.

Deionized water was brought to a slow boil in a pre–weighed erlenmeyer flask on a magnetic stir hot plate. Upon boiling, the flask and water were removed from the heat and capped to prevent dissolution of air back into the water, the flask was set aside to cool. The cooled water was then weighed and its volume determined from density relations. Reagent grade calcium chloride dihydrate ($CaCl_2 \bullet 2H_2O$) was the solute used to make the solution, and has molecular weight of 147.0164 g/mol. The fraction of water in one mole of $CaCl_2 \bullet 2H_2O$ is given by:

$$\% \ water = \frac{36.0304(g/mol)}{147.0164(g/mol)}$$

$$\% \ water = 0.245$$

Therefore, for a solution of 300 ppm $CaCl_2$ the mass–volume relation is:

$$Mass[mg]_{calciumchloride} = (300[mg/l]) \ x \ (Volume[l]_{water}) \ x \ (1.0 + 0.245)$$

A-2.2 PREPARATION OF TCE SOLUTIONS

Three solutions of TCE were prepared at concentrations of 250, 500, and 1000 ppm. The solutions were prepared from standard water and reagent grade trichloroethene. The density of TCE at 25°C is 1.4692 g/cm3, and the volume of TCE for a given dilution can be calculated from the following relation.

$$Volume[\mu l]_{TCE} = \frac{(\ desired\ \ concentration[mg/l]\ \ )x(\ \ Volume[l]_{Water}\ \ )}{1.4692[g/ml]}$$

The solutions were prepared by first weighing each dilution bottle it's cap and septa, and the magnetic stir bar used to mix the solution. Each bottle was then filled with 300 ppm $CaCl_2$ water and sealed with septa and cap. It was critical that no air was present in the system to allow volatilization of the TCE from solution. The full bottle was then weighed and the volume of water calculated from density relations. The amount of TCE for a given dilution was calculated and injected into the bottle using a microsyringe. The bottle was placed on a magnetic stirrer for 48 hours to insure complete dissolution of TCE.

A-3 COLUMN PROPERTIES

A-3.1 PORE VOLUME

The volume of the pores for each column was determined by calculating the volume of the of the sample chamber of the column and subtracting the volume of the porous media.

The volume of the sample chamber was calculated using the equation for the volume of a cylinder:

$$Volume_{cylinder} = \pi\ r^2\ h$$

π = constant

r = radius of cylinder

h = height of cylinder

For the columns used in this study the height and radius were the same for all columns, h = 1.80cm, and the radius = 1.25cm. The diameter of each column was measured using a vernier caliper, and the height set to 1.80cm.

The volume of the porous media was calculated by weighing the empty and packed column, correcting the mass of the porous media for moisture content, and dividing by the mean particle density, see below. Finally, the pore volume can be calculated by subtracting the the volume of the porous media from the volume of the column. The pore volume of each column along with the porosity and bulk density are listed in table A-2.

$$Volume_{Porous\ Media} = \frac{(Mass_{Packed\ Column} - Mass_{Empty\ Column})\ x\ (1.0 - Moisture\ Content\ )}{Mean\ Particle\ Density}$$

$$Volume_{Pores} = Volume_{Column}\ -\ Volume_{Porous\ Media}$$

TABLE A-2

COLUMN PROPERTIES

column	column volume [1]	porous media volume [1]	pore volume [1]	porosity [2]	bulk density [3]
A	8.84	4.58	4.26	0.48	1.30
B	8.84	4.77	4.07	0.46	1.35
C	8.84	4.68	4.16	0.47	1.33

[1] Volumes reported as cm^3

[2] Porosity reported as a decimal fraction

[3] Bulk density reported as g/cm^3

APPENDIX B

B–1 HYDRAULIC CONDUCTIVITY DATA

B–1.1 COLUMN A DATA

B–1.2 COLUMN B DATA

B-1.1 COLUMN A HYDRAULIC CONDUCTIVITY DATA

TABLE B-1

designation	permeant
column A	300 ppm $CaCl_2$
cumulative time(days)	hydraulic conductivity $\times\ 10^{-7}[cm/s]$
0.91	0.9510
1.49	1.0500
1.77	1.1300
2.59	1.0600
2.73	1.0900
3.86	0.8380
4.61	0.8580
5.79	0.9210
7.62	0.4470
8.24	0.6290
9.59	0.6270
10.29	0.6310
11.28	0.6390
12.44	0.6460
14.28	0.6480
15.29	0.6490
16.26	0.6620
17.29	0.6800
17.80	0.6850

TABLE B-1. Stabilization data for column A saturated with 300 ppm $CaCl_2$ aqueous solution.

TABLE B–2

designation	permeant
column A	250 ppm TCE
cumulative time(days)	hydraulic conductivity $\times\ 10^{-6}[cm/s]$
0.20	0.559
0.37	0.611
0.84	0.594
1.35	0.609
1.86	0.630
2.35	0.645
2.90	0.646
3.40	0.681
3.86	0.652
4.42	0.682
4.89	0.710
6.12	0.719
6.92	0.728
7.32	0.708
8.10	0.684
8.41	0.683
8.83	0.610

TABLE B–2. Data for column A saturated with 250 ppm TCE dissolved in 300 ppm $CaCl_2$ aqueous solution.

TABLE B-3

designation	permeant
column A	500 ppm TCE
cumulative time(days)	hydraulic conductivity $\times\ 10^{-6}[cm/s]$
0.92	0.731
2.13	0.678
3.90	0.497
4.41	0.827
5.44	0.652
5.88	0.621
6.85	0.350
7.31	0.607
7.88	0.614
9.04	0.642
10.2	0.635

TABLE B-4

designation	permeant
column A	1000 ppm TCE
cumulative time(days)	hydraulic conductivity $\times\ 10^{-6}[cm/s]$
0.63	0.617
1.22	0.587
1.67	0.561
2.16	0.568
2.67	0.584
3.63	0.552
4.26	0.561
4.71	0.589
6.65	0.595
7.64	0.531
8.65	0.533
9.14	0.566

TABLE B-3 and **B-4**. Data for column A saturated with 500 and 1000 ppm TCE solutions, respectively.

B-1.2 COLUMN B HYDRAULIC CONDUCTIVITY DATA

TABLE B-5

designation	permeant
column B	300 ppm $CaCl_2$
cumulative time (days)	hydraulic conductivity $\times$ $10^{-7}[cm/s]$
0.48	0.364
1.65	0.284
4.50	0.202
6.35	0.126
8.22	0.120
8.92	0.163
9.91	0.110
11.07	0.109
11.91	0.210
13.30	0.0892
14.29	0.109
15.31	0.0888
15.89	0.0788
18.35	0.103
19.28	0.0928
20.30	0.105
21.35	0.0938

TABLE B-5. Stabilization data for column B saturated with 300 ppm $CaCl_2$ aqueous solution.

TABLE B–6

designation	permeant
column B	250 ppm TCE
cumulative time(days)	hydraulic conductivity $\times\ 10^{-7}[cm/s]$
0.37	1.04
1.04	1.02
1.56	0.986
2.32	0.978
2.98	1.07
3.41	1.06
3.79	1.10
4.10	1.05
4.53	1.07
5.08	1.23
5.78	1.09
6.17	0.971
6.98	1.01
7.90	0.940
8.51	0.956
9.04	0.951
9.76	1.01
10.2	1.03

TABLE B–6. Data for column B saturated with 250 ppm TCE solution.

TABLE B-7

designation	permeant
column B	500 ppm TCE
cumulative time (days)	hydraulic conductivity $\times \ 10^{-7}[cm/s]$
0.56	1.02
1.61	1.03
2.45	1.04
3.01	0.921
3.78	0.959
4.42	0.964
5.11	0.972
5.89	0.947
6.51	0.989
7.31	1.02
7.91	0.978
8.48	0.982
9.23	0.987
10.30	1.01

TABLE B-8

designation	permeant
column B	1000 ppm TCE
cumulative time (days)	hydraulic conductivity $\times \ 10^{-7}[cm/s]$
0.25	1.04
1.67	1.05
2.34	0.95
2.74	0.919
3.80	1.06
4.32	1.04
5.08	0.971
5.89	0.965
6.39	1.04
6.92	0.976
7.19	0.983
8.05	0.975
8.83	0.960
9.48	0.958
10.22	0.963

TABLE B-7 and B-8. Data for column B saturated with 500 and 1000 ppm TCE solutions, respectively.

APPENDIX C

C-1 FORTRAN 77 CODES

C-1.1 DATA REORGANIZATION CODE

C-1.2 STATISTICS CODE

C-1.3 PLOTTING CODE

C-1.1 DATA REORGANIZATION CODE

This code allows the extraction of two columns of data from large data sets with option of swapping their order.

```
      PROGRAM REFORM
      REAL V1,V2
C     INTEGER UN(300)
      CHARACTER *20FIL1,FIL2,FORM*50,FORM1*65,ANS*3
      WRITE(6,*)'ENTER THE FILE TO BE REFORMED'
      READ(5,4)FIL1
      OPEN(10,FILE=FIL1)
      REWIND(10)
      WRITE(6,*)'ENTER NEW FILE NAME'
      READ(5,4)FIL2
      OPEN(15,FILE=FIL2)

      WRITE(6,*)'ENTER THE FORMAT OF THE FILE TO BE ALTERED'
      READ(5,4)FORM
      WRITE(6,*)'ENTER FORMAT OF NEW OUTPUT'
      READ(5,4)FORM1
4     FORMAT(A)
      WRITE(6,*)'IS THE X VALUE READ FIRST?(Y/N)'
      READ(5,*)ANS
      IF(ANS .EQ.'Y' .OR. ANS .EQ. 'Y')THEN
        READ(10,*)
        DO 1 I=1,1000
          READ(10,FORM,END=2)V1,V2
C         IF(UN(I) .NE. UN(I-1))THEN
C            WRITE(15,100)
C         ELSE
C         END IF
          WRITE(15,FORM1)V1,V2
1     CONTINUE

      ELSE
        READ(10,*)
        DO 3 I=1,1000
          READ(10,FORM,END=2)V1,V2
C         IF(UN(I) .NE. UN(I-1))THEN
C            WRITE(15,100)
C            ELSE
C         END IF
          WRITE(15,FORM1)V2,V1
3     CONTINUE
      END IF
2     WRITE(15,100)
100   FORMAT(1X,'                    ')
      STOP
      END
```

C-1.2 STATISTICS CODE

This program takes the data from the previous program and calculates various statistical parameters, it also echos the input data and calculates a data set for the best fit line through the data.

```
C***********************************************************************
C        EDWARD F. HAGAN AND PAUL S. DOMSKI                    C
PROGRAM TO FIT A LINE TO A SET OF DATA POINTS USING LEAST
C        SQUARES.  USES IMSL SUBROUTINE RLINE
C        FEB. 2, 1989
C
C***********************************************************************
C
         INTEGER NOBS
C        PARAMETER (NOBS=11)
         REAL BO,B1,STAT(12), XDATA(100), YDATA(100),Y(100)
         EXTERNAL RLINE
         CHARACTER OUTNAM*15,FILNAM*15,OUTFIL*15

C        WRITE(6,*)'ENTER NUMBER OF DATA POINTS'
C        READ(5,*)NOBS
         WRITE(6,*)'ENTER INPUT FILE NAME'
         READ(5,901) FILNAM
         OPEN(UNIT=98,FILE=FILNAM,STATUS='UNKNOWN')
C
         WRITE(6,*)'OUTPUT FILE NAME FOR STAT DATA'
         READ(5,901)OUTNAM
         OPEN(UNIT=99,FILE=OUTNAM,STATUS='UNKNOWN')
901      FORMAT(A)
      WRITE(6,*)'ENTER OUTPUT FILENAME FOR X-Y PLOTTING'
      READ(5,71)OUTFIL
71    FORMAT(A)
      OPEN(10,FILE=OUTFIL)

      NOBS = 0
         DO 55 I=1,1000,1
       READ(98,*,END=46)XDATA(I),YDATA(I)
       WRITE(6,*)XDATA(I),YDATA(I)
       WRITE(10,*)XDATA(I),YDATA(I)
       NOBS = I
 55       CONTINUE
 46   WRITE(10,*)
C
C        CALL IMSL SUBROUTINE
C
         CALL RLINE(NOBS,XDATA,YDATA,BO,B1,STAT)
C
C        SETUP OUTPUT
C
         WRITE(6,10)BO,B1
```

```
            WRITE(99,10)BO,B1
10          FORMAT(//4X,'Y INTERCEPT= ',F7.3,4X,'SLOPE= ',F7.4,/)
            DO 56 I=1,12,1
            WRITE(6,*)STAT(I)
56          CONTINUE
C
            WRITE(99,*)'  MEAN OF XDATA=',STAT(1)
            WRITE(99,*)'  MEAN OF YDATA=',STAT(2)
            WRITE(99,*)'  SAMPLE VARIANCE OF XDATA=',STAT(3)
            WRITE(99,*)'  SAMPLE VARIANCE OF YDATA=',STAT(4)
            WRITE(99,*)'  CORRELATION=',STAT(5)
            WRITE(99,*)' '

            WRITE(99,*)'   X VALUES   Y VALUES'
       WRITE(6,*)'ENTER: X INITIAL; X MAXIMUM; AND INCREMENT'
       READ(5,*)IXIN,IMAX,INCRE
            J=1
            DO 57 I=IXIN,IMAX,INCRE
            K=J
            X=I*1.0
            Y(K)=B1*X+BO
C      Z(K)=(B1*.1+B1)*X+BO
C      F(K)=(B1-.1*B1)*X+BO
            J=K+1
            WRITE(10,*)X,Y(K)
57          CONTINUE
       WRITE(10,*)


C 22        FORMAT(2X,F5.2,4X,F7.3)
            STOP
            END
```

C–1.3 PLOTTING CODE

This program graphically displays the data from the previous two programs using Disspla software.

```
      PROGRAM PLOT

      CALL READXY
      CALL SETPAR
      CALL PLOTEMUP
      STOP
      END
C
C************************************************************************
C
      SUBROUTINE SETPAR
C
C     ROUTINE TO SET DISSPLA PARAMETERS
C
      CHARACTER    HDNG*40,YN*40,XN*40
      INTEGER      STRLEN

      COMMON/PARAMS/ XAXIS,YAXIS,LXNAME(10),LYNAME(10),
     $          LTITL(10),XORIG,YORIG,XMAX,YMAX,XSTP,YSTP,
     $          IINTS,IXTICS,IYTICS,XCYCLE,YCYCLE,RND,GTYPE

      COMMON/XYVALS/ XARAY(80,200),YARAY(80,200),ISYM(80),
     $          IMARK(80),NPTS(80),LPAT(80),NLINES

      XAXIS = 9.0
      YAXIS = 5.0
      IXTICS = 5
      IYTICS = 5

C     LABELLING  TITLE,AXES

      WRITE(*,*)' ENTER X-AXIS LABEL, <CR> FOR NONE'
      READ(*,10) XN
10    FORMAT(A)
      NC = STRLEN(XN)
      XN(NC+1:)='$'
      READ(XN,'(10A4)')(LXNAME(I),I=1,10)

      WRITE(*,*)' ENTER Y-AXIS LABEL, <CR> FOR NONE'
      READ(*,10) YN
      NC = STRLEN(YN)
      YN(NC+1:)='$'
      READ(YN,'(10A4)')(LYNAME(I),I=1,10)

      WRITE(*,*)' ENTER THE PLOT HEADING, <CR> FOR NONE'
      READ(*,10) HDNG
      NC = STRLEN(HDNG)
```

```
      HDNG(NC+1:)='$'
          READ(HDNG,'(10A4)')(LTITL(I),I=1,10)

          RETURN
          END

C
C****************************************************************
C
          SUBROUTINE PLOTEMUP
C
C         USING PARAMETERS SET IN SETPAR TO CREATE THE DISSPLA PLOT.
C         ALSO CALLS READXY TO GET POINTS INTO THE CORRECT ARRAYS.
C

          DIMENSION XRAY(10000),YRAY(10000)
      CHARACTER*1 CH
          COMMON/PARAMS/ XAXIS,YAXIS,LXNAME(10),LYNAME(10),
     $          LTITL(10),XORIG,YORIG,XMAX,YMAX,XSTP,YSTP,
     $          IINTS,IXTICS,IYTICS,XCYCLE,YCYCLE,RND,GTYPE

      COMMON/XYVALS/ XARAY(80,200),YARAY(80,200),ISYM(80),
     $          IMARK(80),NPTS(80),LPAT(80),NLINES

C         INITIALIZE THE PLOTTER OR OUTPUT DEVICE

C     WRITE(*,*)'OUTPUT TO (1) SUN, (2) POPFILE ?'
C     READ(*,*) NZOX
C     IF (NZOX.EQ.1) THEN
C       CALL SUN(0)
C     ELSE
      CALL COMPRS
C     ENDIF
          LE = 77
          OPEN(UNIT=LE,FILE='DISSPLA.MSG')
          CALL SETDEV(LE,LE)

C         SUPPRESS THE PAGE BORDER
          CALL NOBRDR

C     USE DEFAULT SIZES FOR PAGE
      PAGEY=8.5
      PAGEX=11.0
          CALL PAGE(PAGEX,PAGEY)

C     SET AXES SIZES AND DON'T ALLOW ANYTHING OUTSIDE THE PLOT
          CALL AREA2D(XAXIS,YAXIS)
          CALL GRACE(0.)

C     CREATE THE HEADING
      CALL HEADIN(LTITL,100,1.25,1)

C         DEFINE AXIS NUMBERING
      CALL INTAXS
```

```
C          DEFINE DIVISIONS BETWEEN TICK MARKS
           CALL XTICKS(IXTICS)
           CALL YTICKS(IYTICS)


C       LABEL THE AXES
           CALL XNAME(LXNAME,100)
           CALL YNAME(LYNAME,100)


C          THIN OUT THE PLOT FRAME
              CALL THKFRM(0.01)


C       WRITE(*,*)'INPUT (1) FOR USER SET X-AXIS, (2) FOR AUTO :'
C       READ(*,*) NZOX
C       IF (NZOX.EQ.1) THEN
C         WRITE(*,*)'INPUT XORIG,XMAX :'
C         READ(*,*) XORIG,XMAX
C       ENDIF


C       WRITE(*,*)'INPUT (1) FOR USER SET Y-AXIS, (2) FOR AUTO :'
C       READ(*,*) NZOX
C       IF (NZOX.EQ.1) THEN
C         WRITE(*,*)'INPUT YORIG,YMAX :'
C         READ(*,*) YORIG,YMAX
C       ENDIF


C          DEFINE THE UNIT ON THE AXES AND FRAME THE PLOT
        WRITE(*,*)
C       WRITE(*,*)'YMAX AT TOP (Y OR N)?'
C       READ(*,*) CH
C       IF (CH.NE.'Y') THEN
C         YMAX1=YORIG
C         YORIG1=YMAX
C         YMAX=YMAX1
C         YORIG=YORIG1
C       ENDIF

           CALL GRAF(XORIG,'SCALE',XMAX,YORIG,'SCALE',YMAX)
        CALL FRAME


C          REVERSE THE TICKS ON BOTH X AND Y AXES
           CALL XREVTK
           CALL YREVTK


C          PLOT THE POINTS
        DO 100 I=1,NLINES
              CALL FILLAR(I,XARAY,YARAY,XRAY,YRAY,NPTS)
           NPNTS = NPTS(I)
           IF (LPAT(I).EQ.1) CALL DOT
           IF (LPAT(I).EQ.2) CALL DASH
           IF (LPAT(I).EQ.3) CALL CHNDOT
           IF (LPAT(I).EQ.4) CALL CHNDSH
```

```
C          THIS CALL STORES LINE TYPES INSTEAD OF SYMBOLS
           CALL MARKER(ISYM(I))
C            WRITE(*,*)'INPUT (1) FOR STEP, (2) SPLINE, (3) NORMAL :'
C            READ(*,*) NZOX
C            IF (NZOX.EQ.1) CALL STEP
C            IF (NZOX.EQ.2) THEN
C              WRITE(*,*)'INPUT DEGREE OF SMOOTHING :'
C              READ(*,*) TENSN
           TENSN=7.
           CALL RASPLN(TENSN)
C            ENDIF
           CALL CURVE(XRAY,YRAY,NPTS(I),IMARK(I))
C            CALL RESET
100          CONTINUE

C          TERMINATE THE PLOT
           CALL ENDPL(0)
           CALL DONEPL

        RETURN
        END
C***************************************************************
           SUBROUTINE FILLAR(I,XARAY,YARAY,XRAY,YRAY,NPTS)
C
C          ROUTINE TO FILL TWO LINEAR ARRAYS WITH ELEMENTS
C          FROM 2-D ARRAYS
           DIMENSION XARAY(80,200),YARAY(80,200),XRAY(10000)
           DIMENSION NPTS(80),YRAY(10000)
           DO 100 J=1,NPTS(I)
             XRAY(J) = XARAY(I,J)
             YRAY(J) = YARAY(I,J)
100          CONTINUE
           RETURN
           END
C***************************************************************
C
           SUBROUTINE COUNTL
C
C          ROUTINE TO DETERMINE THE NUMBER OF LINES TO BE PLOTTED.
C          READS DATA FILE AS CHARACTER STRINGS TO DO SO,LOOKING FOR
BLANK
C          LINES TO INDICATE NEW LINES.
C
C          INPUT FILE SHOULD ALLREADY BE OPENED AS UNIT 92
C
           CHARACTER DLINE*10
        COMMON/XYVALS/ XARAY(80,200),YARAY(80,200),ISYM(80),
     $              IMARK(80),NPTS(80),LPAT(80),NLINES

           NLINES = 0
```

```
10        NPNTS = 0
11            READ(92,901,END=99)DLINE
              IF(DLINE.NE.'          ') THEN
                NPNTS = NPNTS + 1
                GOTO 11
              ENDIF
              NLINES = NLINES + 1
          NPTS(NLINES) = NPNTS
          WRITE(*,*)' LINE ',NLINES,' HAS ', NPTS(NLINES),' POINTS'
              GOTO 10
99        WRITE(*,*)' THERE ARE ',NLINES,' LINES FOR PLOTTING'
              REWIND (UNIT=92)
              RETURN
901           FORMAT(A)
              END
C*********************************************************************
C
          SUBROUTINE MINMAX
C
C         READS INPUT DATA FILE AND DETERMINES NUMBER OF LINES TO PLOT
C         AND MIN AND MAX VALUES FOR FIRST AND SECOND VALUES TO BE
PLOTTED.
C
          COMMON/PARAMS/XAXIS,YAXIS,LXNAME(10),LYNAME(10),
     $          LTITL(10),XORIG,YORIG,XMAX,YMAX,XSTP,YSTP,
     $          IINTS,IXTICS,IYTICS,XCYCLE,YCYCLE,RND,GTYPE

        COMMON/XYVALS/ XARAY(80,200),YARAY(80,200),ISYM(80),
     $          IMARK(80),NPTS(80),LPAT(80),NLINES
C
C         INPUT FILE SHOULD ALLREADY BE OPENED AS UNIT 92

          IRD=92
          XMAX = 0.
          YMAX = 0.
          XMIN = 1.E+32
          YMIN = 1.E+32

10        READ(IRD,*,END=99)X,Y
          IF(X.GT.XMAX) XMAX=X
          IF(X.LT.XMIN) XMIN=X
          IF(Y.GT.YMAX) YMAX=Y
          IF(Y.LT.YMIN) YMIN=Y
          GOTO 10
99        REWIND (UNIT=92)
          XORIG=XMIN
          YORIG=YMIN
          RETURN
          END
C
```

```
C*****************************************************************************
C
          SUBROUTINE READXY
C
C         ROUTINE TO READ IN SETS OF POINTS AND SET PLOTTING PARAMETERS
C
          CHARACTER FILNAM*10,BLANK*10,LPTEMP*1
          COMMON/XYVALS/ XARAY(80,200),YARAY(80,200),ISYM(80),
     $             IMARK(80),NPTS(80),LPAT(80),NLINES

      WRITE(*,*)' ENTER DATA FILE NAME'
      READ(*,10) FILNAM
   10    FORMAT(A)
      OPEN(UNIT=92,FILE=FILNAM,STATUS='OLD',ACCESS='READONLY')

C     DETERMINE NUMBER OF LINES, NUMBER OF POINTS IN EACH LINE,
C        MINIMUM AND MAXIMUM VALUES FOR RANGE OF X AND Y
         CALL COUNTL
         CALL MINMAX

         REWIND(UNIT=92)

      DO 100 I=1,NLINES
C      READ THE X,Y PAIRS
      READ(92,*) (XARAY(I,J),YARAY(I,J),J=1,NPTS(I))
         READ(92,901,END=101)BLANK

         WRITE(*,*)
         WRITE(*,*)' FOR LINE ',I,' DO YOU WANT'
      WRITE(*,*)' +I - POINTS CONNECTED AND A SYMBOL EVERY',
     $             ' I"TH POINT'
      WRITE(*,*)' -I - POINTS NOT CONNECTED AND A SYMBOL EVERY',
     $             ' I"TH POINT'
         WRITE(*,*)'  0 = POINTS CONNECTED WITH NO SYMBOLS DRAWN'
      READ(*,*)IMARK(I)

      IF(IMARK(I).NE.0) THEN
       WRITE(*,*)' ENTER SYMBOL TYPE FOR LINE ',I
          WRITE(*,*)'  0 - BOX'
          WRITE(*,*)'  1 - OCTAGON'
          WRITE(*,*)'  2 - TRIANGLE'
          WRITE(*,*)'  3 - +'
          WRITE(*,*)'  4 - X'
          WRITE(*,*)'  5 - DIAMOND'
          WRITE(*,*)'  6 - DEL'
          WRITE(*,*)'  7 - BOXED X'
          WRITE(*,*)'  SEE P.17 OF POCKET GUIDE FOR REST'
      READ(*,*)ISYM(I)
         ENDIF

         IF(IMARK(I).GE.0) THEN
          WRITE(*,*)' ENTER LINE PATTERN FOR LINE',I
```

```
        WRITE(*,*)' <CR> - SOLID'
     WRITE(*,*)'    1 - DOTTED '
        WRITE(*,*)'   2 - DASHED '
        WRITE(*,*)'    3 - CHAIN DOTTED'
        WRITE(*,*)'    4 - CHAIN DASHED'
        READ(*,901)LPTEMP
        IF(LPTEMP.EQ.' ')THEN
              LPAT(I)=0
        ELSEIF(LPTEMP.EQ.'1')THEN
              LPAT(I)=1
        ELSEIF(LPTEMP.EQ.'2')THEN
              LPAT(I)=2
        ELSEIF(LPTEMP.EQ.'3')THEN
              LPAT(I)=3
        ELSEIF(LPTEMP.EQ.'4')THEN
              LPAT(I)=4
        ENDIF
     ENDIF

100   CONTINUE

        CLOSE(UNIT=92)
101   RETURN

99    FORMAT(2F15.3)
901      FORMAT(A)
      END

      INTEGER FUNCTION STRLEN(STRING)

      CHARACTER*(*) STRING
      INTEGER COUNT,MAXLEN
      LOGICAL PRTABL

      MAXLEN = LEN (STRING)
      DO 100 COUNT=MAXLEN,0,-1
      IF (COUNT.EQ.0) THEN
         STRLEN = COUNT
         RETURN
      ELSE IF (PRTABL(STRING(COUNT:COUNT))) THEN
         STRLEN = COUNT
         RETURN
      ENDIF
100   CONTINUE
      END

      LOGICAL FUNCTION PRTABL(CHAR)

      CHARACTER*1 CHAR

      IF (ICHAR(CHAR) .GE. ICHAR('!') .AND.
1     ICHAR(CHAR) .LE. ICHAR('~')) THEN
```
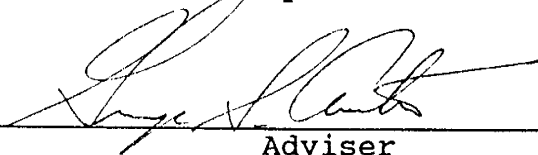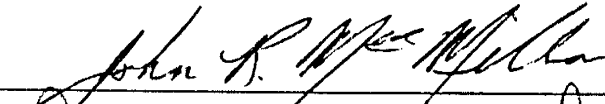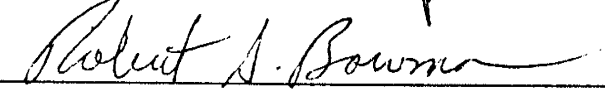
```
      PRTABL = .TRUE.
ELSE
      PRTABL = .FALSE.
ENDIF
RETURN
END
```

This thesis is accepted on behalf of the faculty
of the Institute, by the following committee:

_____
                    Adviser

_____

_____

_____

_____

_____ July 13, 1989 _____
                    Date